Energy Equip. Sys./ Vol. 14/No. 1/March 2026/ 1-32

ENERGY EQUIPSYS

Energy Equipment and Systems

www.energyequipsys.com

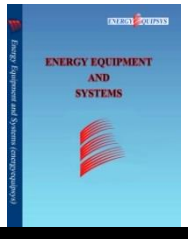

Integrated techno-environmental-economic and thermal assessment of a solar-powered HDH-RO-battery desalination system

Manuscript Type

Research Paper

Authors

Alireza Asgharzadeh Karamshahlu[a]
Mohammad Hassan Saidi[a*]
Hooman Bahman Jahromi[a]
Mohammad Behzadi-Sarok[a]

[a] Center of Excellence in Energy Conversion (CEEC), School of Mechanical Engineering, Sharif University of Technology, Tehran, Iran

Article history:
Received: 1 November 2025
Revised: 5 December 2025
Accepted : 6 January 2026

ABSTRACT

Ensuring a continuous freshwater supply in off-grid regions is challenging due to the intermittent nature of renewable energy and the high energy demand of desalination. This study presents a solar-powered hybrid humidification-dehumidification and reverse osmosis (HDH-RO) desalination system integrated with lithium-ion (NMC) battery storage for fully autonomous 24-hour operation. A coupled techno-economic and thermal modeling framework was developed, linking HOMER Pro (v3.18.3) optimization with ANSYS Fluent (2022R2) transient thermal simulations of the battery pack to ensure cost-effective performance and verify battery thermal safety. The optimized configuration comprising a 7.5 kW photovoltaic array, eight 94 Ah batteries, and a 1.68 kW converter delivers a steady 0.7 kW load, producing freshwater at a levelized cost of 0.95 $/m^3 and a net present cost of 25,946 $, 24% lower than a diesel-powered system. Thermal analysis showed a maximum 6.3 K temperature rise in the battery cells over 24 hours, confirming safe operation without active cooling. The proposed system demonstrates its practical feasibility for implementation in Hengam Island, representing a viable and sustainable solution for continuous, off-grid freshwater production in coastal regions. In addition to powering desalination, the PV-battery configuration generates surplus clean electricity, serving as a dual-purpose energy-water system that substantially reduces diesel dependence and emissions, achieving an annual reduction of about 9.8 tons of air pollutants. The results highlight a scalable, integrated, and zero-emission energy-water system for sustainable development in isolated island regions.

Keywords: Solar-Powered Desalination, Hybrid HDH-RO System, Lithium-Ion (NMC) Battery Storage, Techno-Economic Analysis, Off-Grid Freshwater Production.

1. Introduction

Freshwater scarcity has become a critical global challenge, with projections indicating that nearly 60% of the world's population may face water shortages by 2050 [1,2]. Given that more than 96% of Earth's water resources are saline, desalination has emerged as an essential

* Corresponding author: Mohammad Hassan Saidi
Center of Excellence in Energy Conversion (CEEC), School of Mechanical Engineering, Sharif University of Technology, Tehran, Iran
Email: saman@sharif.edu

solution. However, it remains highly energy-intensive, requiring 3-15 kWh of electricity per cubic meter of freshwater produced [3–6]. Renewable energy sources, particularly solar energy, offer a promising pathway to reduce operational costs, mitigate environmental impacts, and enable off-grid desalination in remote regions [6,7]. Among desalination technologies, reverse osmosis (RO) is widely adopted due to its high efficiency and water quality. In contrast, hybrid energy systems that integrate solar, wind, and storage technologies have demonstrated strong potential in enhancing reliability and sustainability for isolated communities [8]. Diesel-based electricity generation, commonly used in remote locations, is both costly and environmentally harmful, whereas hybrid solar-wind-hydrogen systems and tools such as HOMER Pro have shown that renewable-integrated configurations can effectively reduce both emissions and levelized energy cost [9,10].

The integration of photovoltaic (PV) systems with small-scale RO desalination plants is technically and economically viable, especially in coastal regions with abundant solar resources [11]. However, while hybrid power systems equipped with energy storage improve reliability, the inclusion of batteries often increases system cost, highlighting the importance of optimized sizing and control strategies [12]. Recent techno-enviro-economic studies on large-scale renewable-powered RO systems demonstrate that combining multiple renewable sources with energy storage can significantly reduce the levelized cost of water (LCOW) while enhancing sustainability and operational reliability [13]. Furthermore, replacing diesel generators with hybrid renewable energy systems (HRES) has consistently been shown to reduce operational expenditures and greenhouse gas emissions in off-grid regions [14]. Experimental and theoretical investigations support these findings. Ramazanian et al. [15] achieved 150 L/day of freshwater using a solar-battery hybrid system with energy recovery; Abdulrahman et al. [16] demonstrated improved RO performance through solar-based feedwater preheating; Monnot et al. [17] reported a 65% increase in recovery rate when batteries were integrated; and Al-Madawi et al. [18] optimized solar-wind-diesel–battery systems to reduce cost and maximize renewable fraction. Ahmed Ali et al. [19] evaluated a hybrid PV-wind-hydrogen-battery system for powering an RO unit and demonstrated that integrating multiple renewable sources can substantially reduce energy costs while achieving near-zero emissions, underscoring the importance of optimized hybrid configurations for desalination applications.

Humidification-dehumidification (HDH) desalination systems have also attracted attention for their simplicity, low capital costs, and operational flexibility, making them suitable for remote and off-grid regions. Performance improvements in HDH systems through heat pump integration and parametric optimization have been well documented [20–22]. Hybrid HDH-RO configurations, which combine the advantages of both technologies, offer reduced energy consumption, higher freshwater quality, and improved overall efficiency compared with standalone systems [23,24].

Recent advancements in hybrid renewable desalination systems emphasize the importance of integrating solar, wind, and biomass resources to enhance reliability and reduce the levelized cost of energy [25–29]. Several studies across Egypt, islanded regions, and arid climates confirm the viability of PV-wind desalination systems [30–33]. Building-integrated PV approaches further alleviate dependence on unstable grids (34). PV-driven RO systems equipped with energy recovery devices improve both productivity and energy efficiency [35], while solar-powered electrodialysis reversal (EDR) and RO systems are identified as effective options for high-salinity water treatment [36]. Off-grid PVRO systems have been proven technically and economically feasible in Iran, with optimization-based approaches enhancing reliability and cost-effectiveness [37]. Additional research demonstrates that hybrid renewable configurations can significantly increase RO performance in remote and semi-arid regions [38–41]. Optimized grid-connected PV systems in Saudi Arabia have shown improved performance and cost savings [42]. At the same time, MATLAB/SIMULINK-HOMER Pro hybrid validations confirm the potential to reduce both cost and storage requirements [43].

Hybrid PV-wind systems have also been shown to mitigate environmental impacts and decrease energy expenses across residential and institutional settings [44,45]. Furthermore, optimization studies on large-scale seawater RO plants indicate that intermittent operation of oversized RO units can minimize both energy cost and emissions [46]. Innovative low-carbon desalination concepts that combine multistage flash processes, photocatalytic water splitting, and fuel cells demonstrate the potential for simultaneous freshwater, hydrogen, and electricity production [47]. Hybrid solar PV, power-to-gas, and HDH-RO systems have likewise exhibited high operational efficiency and effective CO_2 utilization [48]. Comparative evaluations of HDH configurations reveal that the choice of working fluid and system configuration, open-water, closed-air, or hybrid HDH-RO, significantly influences exergetic efficiency and freshwater cost [49–51]. Bubble-column HDH systems enhanced by water-source heat pumps and analyzed using the Poppe method have shown improvements in gain output ratio (GOR), productivity, and cost-effectiveness [52–54].

Lithium-ion batteries, widely recognized for their high energy density, long cycle life, and rapid response, have become a key component in renewable-powered desalination systems [55]. However, their thermal behavior is critically dependent on temperature gradients, charge-discharge cycles, and cooling strategies [56–59]. Previous studies on battery thermal management systems (BTMS) reveal that indirect cooling methods, such as bottom-plate cooling, perform effectively at low discharge rates but become less efficient under high loads, while air cooling suffers from limited convective heat transfer. In comparison, liquid-based and two-phase immersion cooling systems offer better temperature uniformity and thermal control [60]. Coupled electrochemical-thermal models further indicate that temperature, current rate, and cooling conditions play decisive roles in battery safety and longevity [61]. These findings highlight the essential need for effective thermal management to ensure stable, reliable operation of renewable-powered systems that rely heavily on lithium-ion batteries.

Despite notable progress in renewable-powered desalination, most existing studies have examined either humidification-dehumidification (HDH) or reverse osmosis (RO) independently, providing limited insight into the integrated performance of the hybrid HDH-RO cycle. Moreover, prior research has predominantly focused on the desalination process itself, with insufficient attention to the holistic design, energy supply integration, long-term techno-economic assessment, and off-grid operability of such systems. Although PV-battery configurations are widely adopted for renewable energy supply, few previous works have incorporated a high-fidelity thermal analysis of lithium-ion batteries, despite the well-established influence of temperature on degradation, efficiency loss, and reduced lifetime [56–58,61]. The absence of battery thermal modeling introduces significant uncertainty in system reliability and life-cycle cost, particularly for remote and off-grid applications where continuous 24-hour operation is required. Consequently, a comprehensive framework that simultaneously integrates solar energy system design, techno-economic optimization, environmental assessment, and detailed thermal evaluation of the storage unit for a hybrid HDH-RO desalination system remains largely unexplored. This study addresses this critical research gap by developing and evaluating a fully autonomous PV-Battery-(HDH-RO) system capable of delivering continuous freshwater production with zero direct/operational emissions. Table 1 summarizes the most relevant works reported in the literature review.

The novelty of this study lies in the development of a fully integrated, solar-powered HDH-RO desalination system capable of delivering continuous 24-hour freshwater production through a combined techno-economic and thermal framework. Unlike previous works that treat batteries as secondary backup units, this study incorporates lithium-ion batteries as a primary operational component and performs a high-fidelity thermal analysis to ensure safe, reliable, and cost-effective nighttime operation, an essential requirement for remote and arid regions.

Table 1. Summary of prior studies in the literature.

Author	Desalination	Power Configuration	Region / Site Type	Summary of the Work Done
Abdullah et al. (24)	HDH-RO	PV-Battery	Saudi Arabia	Solar-powered HDH-RO system achieved 535 L/day with 0.63 $/m³ water cost, outperforming standalone units
Jamil et al. (50)	HDH-RO	PV	Pakistan	Exergo-economic study showed HDH-RO with pressure exchanger and solar heater had the best performance, lowest cost (0.12 $/m³)
Ramazanian et al. (15)	RO	PV-WT-Battery	Rural and remote areas	The hybrid PV-WT-Battery-RO system produced 150 L/day (TDS = 120 ppm) with the highest efficiency for the rural Ilam region.
Abdelrahman et al. (16)	RO	PV	Egypt	Solar-powered RO with solar preheating reduced energy use, increased freshwater yield, and lowered emissions.
Monnot et al. (17)	RO	PV-(with and without Battery)	India	Optimized PV-RO with a double-stage setup achieved 65% recovery and lower cost; batteries further reduced costs.
Elmaadawy et al. (18)	RO	PV-Wind-DG-Battery	Remote (off-grid)	Hybrid solar-wind-diesel-battery system (1500 m³/day RO) cut costs and emissions, raising renewable share to 81.5%

The main contributions of this research are as follows:

- A new PV-Battery-(HDH-RO) architecture enabling fully autonomous, zero-emission freshwater production across day-night cycles.
- Development of an integrated techno-economic and thermal assessment framework that simultaneously evaluates the life-cycle cost, reliability, and thermal behavior of the entire solar-battery-(HDH-RO) system.
- A detailed 3D thermal simulation of lithium-ion batteries using ANSYS Fluent, addressing overheating risks that are rarely considered in renewable-powered desalination studies.
- Demonstration of significant economic and environmental benefits compared with diesel-based systems, highlighting the system's suitability for isolated coastal and desert communities.
- Provision of a scalable methodology for designing future large-capacity HDH-RO desalination plants powered solely by renewable energy.

Because the hybrid HDH-RO desalination configuration represents an integrated cycle with improved overall performance compared with standalone HDH or RO, it was selected for this study. In particular, the HDH-RO hybrid is generally more energy-efficient in the sense that, for a comparable energy input, it can produce more freshwater than the separate HDH or RO cycles due to its higher overall effectiveness. Since the main objective of this work is to design and optimize the power-supply system for continuous desalination, the HDH-RO cycle was adopted to enable a more optimal and practically relevant energy-water solution.

Nomenclature

C	Cost ($)
COE	Cost of Energy ($)
c_p	Specific heat capacity (J/(kg . K)
CPL	Cost Per Liter ($/L)
f	Inflation rate (%)
i	Real interest rate (%)
i'	Nominal interest rate (%)
k	Thermal conductivity (W/m.K)
LCOE	Levelized Cost of Energy ($/kWh)
LCOW	Cost of freshwater production per cubic meter ($/m^3)
n	Project lifetime
$\dot{q}$	Heat generation (W/m^3)
SOC	State of charge (%)
T	Temperature (K,˚C)
TPC	Total project cost ($)
TPW	Total produced freshwater (m^3)
V	Voltage (V)

Greek Letters

ρ	Material density (kg/ m^3)
σ	Electrical conductivity (S/m)
ϕ	Electrical potential (V)

Subscripts

+	positive electrode
-	negative electrode
abuse	heat generation under abnormal conditions
ACC	Annualized capital cost
AOM	Annual operation and maintenance
ARC	Annualized replacement cost of system components
ECH	Heat generation due to electrochemical reactions
short	Heat generation caused by internal short circuits

Abbreviations

C-rate	Charge/Discharge rate
CRF	Capital recovery factor
CWOA	Closed-Water Open-Air configuration
EDR	Electrodialysis Reversal
EES	Electrical Energy Storage
GOR	Gain Output Ratio
HDH	Humidification-Dehumidification
HOMER	Hybrid Optimization Model for Multiple Energy Resources
HP	Heat Pump
HPWS	Hybrid Photovoltaic-Wind System
HRES	Hybrid Renewable Energy System
NMC	Nickel Manganese Cobalt
NPC	Net Present Cost
NZLD	Near Zero Liquid Discharge
PV	Photovoltaic
PVRO	Photovoltaic Reverse Osmosis
PWS	Photocatalytic Water Splitting
RES	Renewable Energy Sources
RO	Reverse Osmosis

2. Methodology

This study presents the design and evaluation of a hybrid desalination system that combines reverse osmosis with humidification-dehumidification processes, powered entirely by renewable energy. The primary objective is to provide continuous electricity to the HDH-RO unit during the daytime using photovoltaic panels and to store it in batteries at night. The study site was analyzed for solar energy potential, load demand, and environmental conditions, and the technical constraints associated with renewable energy technologies and the local climate were identified. Based on this assessment, the most suitable energy generation and storage technologies were selected and modeled in HOMER Pro.

The modeling and optimization process aimed to minimize the net present cost, reduce energy production expenses, and lower carbon emissions. Several system configurations were compared according to these metrics, and the optimal option was identified from technical, economic, and environmental perspectives. The chosen configuration was then further evaluated with respect to its operational performance, economic indicators, and environmental impacts. Additionally, a sensitivity analysis was conducted to examine the system's reliability under variations in solar radiation, load fluctuations, and potential changes in equipment costs. Overall, the study proposes an optimized and sustainable configuration as a more economical, environmentally friendly, and reliable alternative to conventional diesel-powered desalination systems.

Tehran was selected as the reference location for the simulation because the physical HDH-RO desalination prototype developed in this study was installed and tested in Tehran. Therefore, using local meteorological data ensures that the numerical analysis reflects the actual operating conditions of the experimental system. Although the simulation corresponds to Tehran's climate, the design concept and operating behavior of the proposed PV-Battery-(HDH-RO) configuration remain applicable to other high-solar-resource regions such as Hengam Island.

2.1. Hybrid humidification-dehumidification and reverse osmosis desalination unit

This section describes and analyzes the components of the laboratory-scale hybrid HDH-RO desalination cycle used in the experimental setup. Figure 1 presents the humidification, dehumidification, and reverse osmosis unit located in the air-conditioning laboratory. Experimental data for the hybrid HDH-RO system were collected from the setup installed at the Faculty of Mechanical Engineering, Sharif University of Technology, Tehran, Iran (35°42.4′ N, 51°21′ E). The measurements indicate that the system can produce 155 liters of freshwater per hour.

(a) (b)

Fig. 1. (a) Humidification-dehumidification desalination unit with a heat pump, (b) Reverse osmosis desalination unit.

The humidification-dehumidification unit incorporates a heat pump, which significantly enhances moisture absorption and condensation when operated in coordination with the HDH cycle. Owing to their high coefficient of performance, heat pumps play a key role in improving the efficiency of thermal desalination processes. A schematic diagram of the hybrid HDH-RO system is shown in Fig. 2, and the technical specifications of the desalination setup are summarized in Table 2. The capital cost and O&M cost of the hybrid HDH-RO desalination unit are $1,500 and $100, respectively, and its lifetime is 20 years.

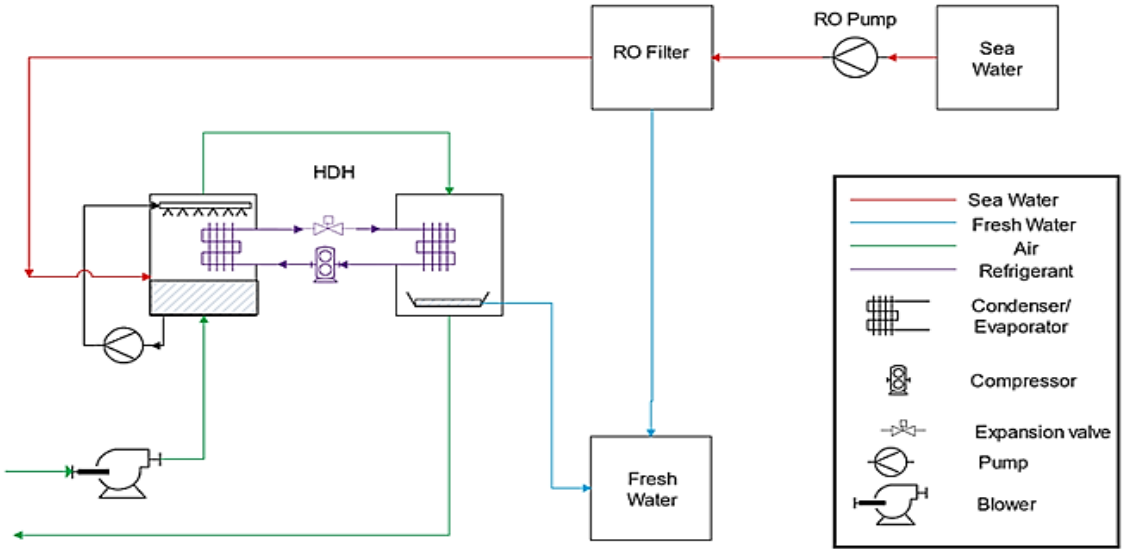

Fig. 2. Schematic of the hybrid humidification-dehumidification and reverse osmosis desalination system.

Table 2. Specifications of the hybrid humidification, dehumidification, and reverse osmosis desalination system.

HDH-RO components	
Raw water feed flow	370 L/h
Plant hourly permeate flow	155 L/h
RO feed pressure	11 bar
Production ratio	42%
Feedwater design temperature	298K
Feedwater TDS	10000 mg/L
Brine water (HDH input)	15000 mg/L
Operation period	24 hr/day
Freshwater output quality	400 mg/L
Peak power demand	0.7 kW
Average power demand	0.7 kW
Energy consumption	16.8 kWh/day
Refrigerant	R134a

2.2. Description of Input Parameters

The subsequent subsections provide a detailed description of the input parameters utilized in the HOMER Pro software, covering aspects such as load demand evaluation and the performance analysis of renewable energy resources.

2.2.1. Load Demand of the Hybrid Humidification-Dehumidification and Reverse Osmosis Desalination System

According to Table 2, the hybrid HDH-RO desalination system requires an electrical input of 700 W. The power consumption of each component in the hybrid cycle is summarized in Table 3. The system operates continuously throughout the year, consuming 700 W over a 24-hour period. This constant demand results from the steady operating conditions of the RO pump, heat pump modules, and air blower. In a controlled laboratory environment where air temperature and humidity remain stable, the heat pump operates at optimal conditions, enabling the system to achieve maximum freshwater production at this power level.

Although the components gradually warm up during operation, causing slight changes in their performance, these variations are minimal and therefore neglected. The system's total daily energy requirement is 16.8 kWh. This constant load was incorporated into the HOMER Pro model to evaluate and optimize the system's ability to maintain a stable, uninterrupted power supply.

Solar radiation data for Tehran were obtained from the reliable NASA database [62]. Figure 3(a) illustrates the annual solar irradiance and clearness index, which range from 2.73 kWh/m²/day in January to 2.38 kWh/m²/day in December, with a maximum of 7.35 kWh/m²/day in July. The annual mean solar irradiance is 4.89 kWh/m²/day, accompanied by a clearness index of 0.585. Solar intensity remains relatively high from April to September, then declines noticeably from October to February. The annual temperature profile for Tehran is shown in Fig. 3(b).

Table 3. Power consumption of the components of the hybrid humidification, dehumidification, and reverse osmosis desalination system.

Item	Power (W)
High-pressure pump	250
Air blowers	150
Heat pump components	300

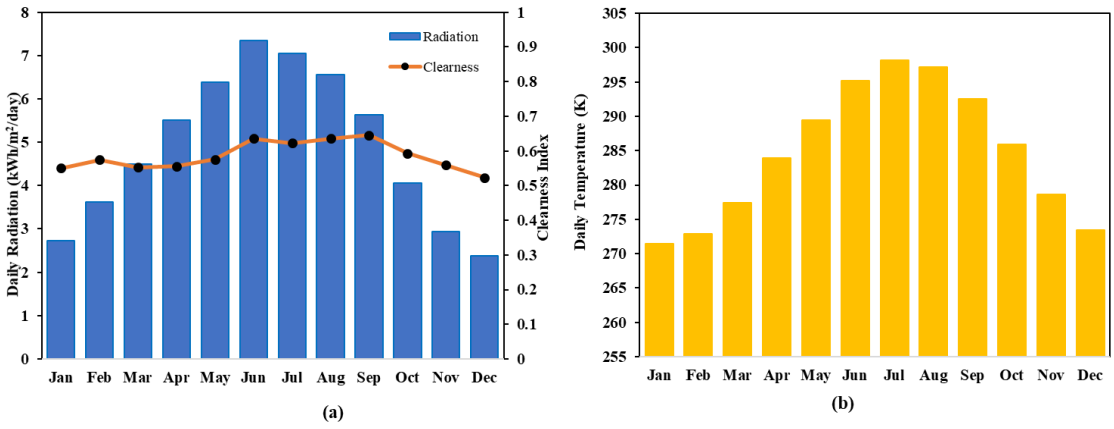

Fig. 3. (a) Annual solar irradiance and clearness index in Tehran, (b) Annual air temperature profile in Tehran.

2.3. System Structure and Component Specifications

The energy configuration proposed in this study operates as an off-grid system comprising photovoltaic panels and battery storage, supplying power to the hybrid HDH-RO desalination setup (Fig. 4). The PV array serves as the primary energy source during the daytime (7:00 AM–6:00 PM), while simultaneously charging the battery bank. At night (6:00 PM–7:00 AM), when solar radiation is unavailable, the battery system provides backup power, ensuring continuous operation of the desalination process and uninterrupted freshwater generation over a 24-hour period. The technical and economic characteristics of the components used are summarized in Table 4.

Table 4. Technical and economic specifications of the system components.

PV array	
Technology	AU Optronics333PM096B00_333
Peak power (W)	333
Efficiency (%)	20.4
Capital cost ($)	637.2
Replacement cost ($)	637.2
Operation & maintenance cost ($/year)	12.7
Derating factor (%)	85
Life time (year)	25
Nominal operating cell temperature (K)	318
Converter	
Technology	CyboEnergy Off-Grid C1-Mini-1000
Power (kW)	1
Efficiency (%)	96
Capital cost ($)	124.6
Replacement cost ($)	124.6
Life time (year)	10
Battery	
Technology	SENEC.Home V3 hybrid 5 Storage Component
Nominal capacity (kWh)	4.84
Maximal capacity (Ah)	94
Voltage (V)	51.5
Capital cost ($)	1500
Replacement cost ($)	1500
Operation & maintenance cost ($/year)	10
Minimum state of charge (%)	10
Life time (year)	20

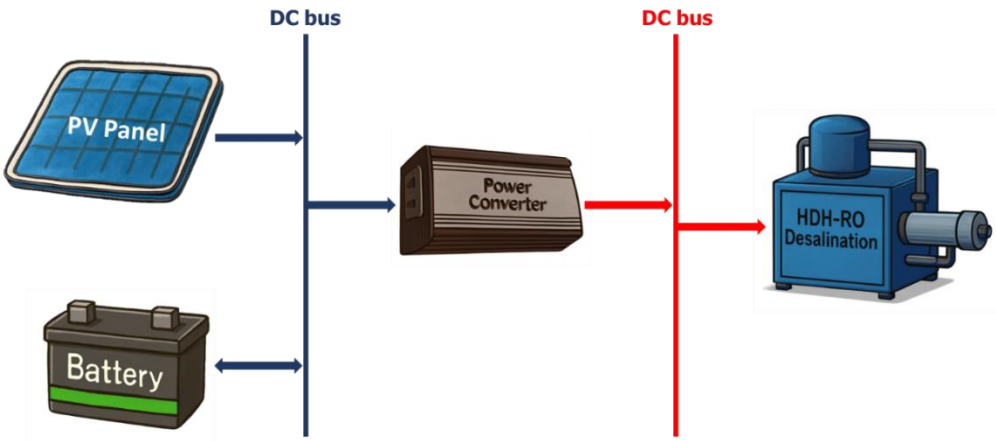

Fig. 4. Configuration of the energy system developed in the present study.

2.4. Model Optimization Procedure and Criteria

In this study, a techno-enviro-economic framework is developed to design a PV-battery-powered HDH-RO desalination system capable of continuous 24-hour operation. The optimization process aims to minimize both the net present cost (NPC) and the cost of energy (COE), while accounting for PV array capacity, battery storage size, and converter power rating. The overall workflow used to identify the optimal configuration is illustrated in the flowchart shown in Fig. 5.

The analysis incorporates site-specific solar radiation data, hourly load demand, and predefined technical and economic parameters. In HOMER Pro, the PV system is initially simulated to satisfy the energy demand, with surplus daytime energy directed to charge the battery bank. The stored energy is then discharged at night to ensure uninterrupted system operation. After conducting an energy balance and a comprehensive techno-enviro-economic assessment, HOMER Pro evaluates and ranks all feasible design alternatives. The configuration with the lowest NPC is subsequently selected as the optimal solution.

2.5. Evaluation Criteria

To assess the effectiveness of the proposed system, several technical and economic parameters were considered. The main evaluation indicators are as follows:

The net present cost reflects the overall expenditure, including investment, operational, and maintenance costs throughout the system's operational lifespan. Equation (1) is employed to determine the net present cost of the system [30],

$$NPC = \frac{C_{ACC} + C_{ARC} + C_{AOM}}{CRF\left(i', n\right)} \tag{1}$$

where, C_{ACC}, C_{ARC}, C_{AOM}, $CRF(i', n)$, i', and n denote the annualized capital and replacement costs, annual operating and maintenance expenses, capital recovery factor, nominal interest rate, and total project lifetime, respectively. Equation (2) is used to compute the capital recovery factor [30],

$$CRF\left(i, n\right) = \frac{i\left(1+i\right)^{n}}{\left(1+i\right)^{n} - 1} \tag{2}$$

HOMER Pro applies the real interest rate in its computations, derived [30],

$$i = \frac{i' - f}{1 + f} \tag{3}$$

where, i, i', and f Correspond to the real interest rate, the nominal interest rate, and the inflation rate, respectively.

Cost of energy: This cost represents the average cost of producing each kilowatt-hour of electricity by the system. It is calculated by [30]

$$COE = \frac{C_{ACC} + C_{ARC} + C_{AOM}}{E_{AEC}} \tag{4}$$

where E_{AEC} is the annual electricity supplied. As defined, the cost of freshwater generation in the hybrid humidification-dehumidification

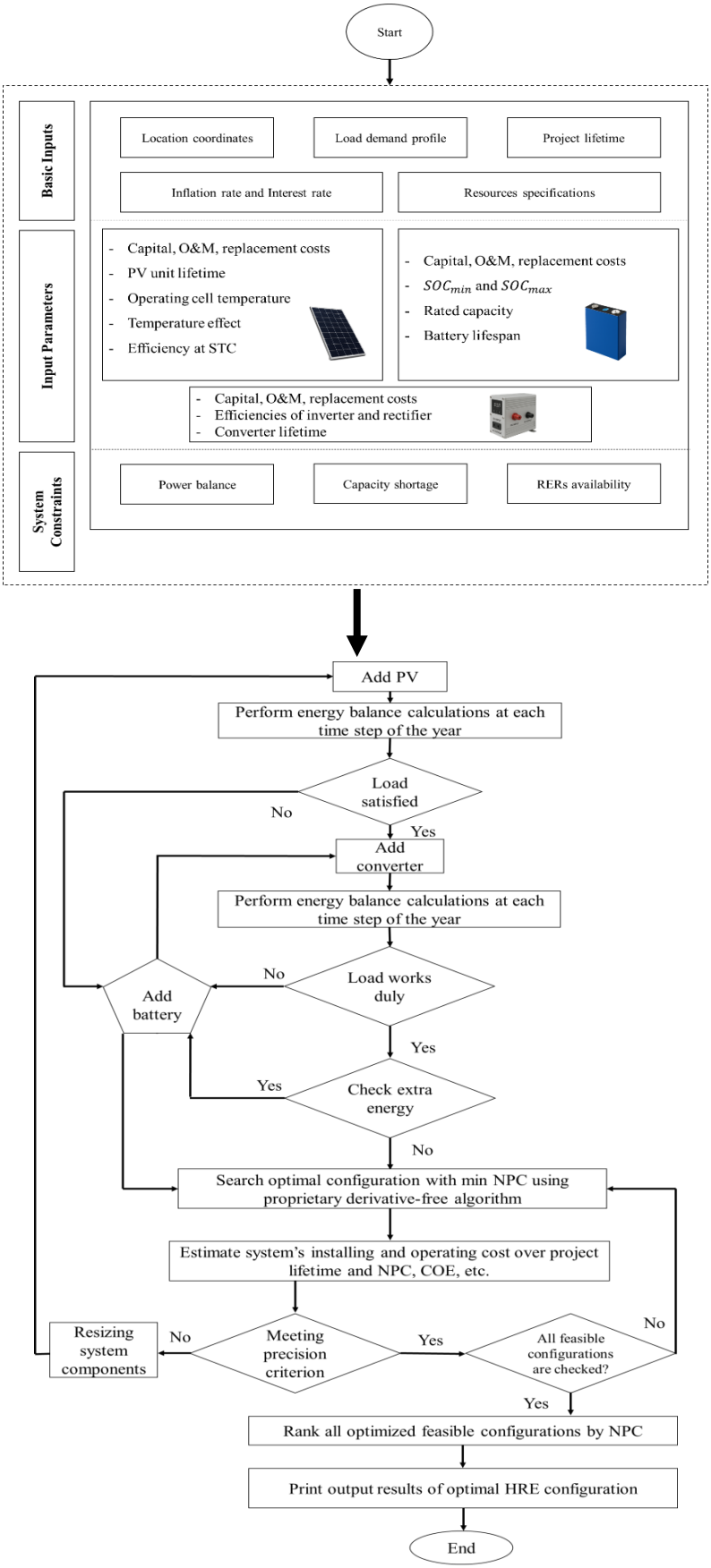

Fig. 5. Optimization process in HOMER Pro for selecting the optimal configuration.

and reverse osmosis desalination system is obtained with

$$LCOW = \frac{TPC}{TPW} \tag{5}$$

where LCOW, TPC, and TPW denote the levelized cost of water per cubic meter, the overall project expenditure, and the total volume of freshwater produced, respectively.

To evaluate the techno-economic and environmental benefits of the proposed solar-battery-powered hybrid HDH-RO desalination system, a diesel-only reference configuration was also modeled in HOMER Pro. In this baseline scenario, the entire electrical load of the desalination unit is supplied by a conventional diesel generator. The simulation assumes a diesel fuel price of $0.60 per liter, an initial capital cost of $500, and a replacement cost of $400. HOMER automatically estimated operation and maintenance expenses based on standard generator performance characteristics.

The project lifetime, nominal interest rate (23%), and inflation rate (22.2%) were kept consistent with those applied in the hybrid renewable system to enable a fair comparison. The results of this diesel-only baseline case were then compared with the solar-battery configuration in terms of Net Present Cost (NPC), Levelized Cost of Energy (LCOE), and Levelized Cost of Water (LCOW). This comparative assessment provides a clear evaluation of the economic feasibility and environmental advantages of replacing fossil-fuel-based power generation with renewable energy in off-grid desalination applications.

2.6. Numerical Method for Battery Thermal Analysis

This section provides a detailed explanation of the approach used to perform the thermal analysis of the battery unit.

2.6.1. Governing Equations of the Battery

The governing equations for lithium-ion batteries are expressed as follows. Equation (6) represents heat transfer in the battery [63]

$$\frac{\partial \rho C_p T}{\partial t} - \nabla.\left(k \nabla T\right) = \sigma_+ \left|\nabla \phi_+\right|^2 + \sigma_- \left|\nabla \phi_-\right|^2 + \dot{q}_{Ech} + \dot{q}_{short} + \dot{q}_{abuse} \tag{6}$$

Equation (7) governs the current transport in the positive electrode, while Eq.(8) governs the current transport in the negative electrode [60]

$$\nabla.\left(\sigma_+ \nabla \phi_+\right) = -\left(j_{Ech} - j_{short}\right), \tag{7}$$

$$\nabla.\left(\sigma_- \nabla \phi_-\right) = j_{Ech} - j_{short}. \tag{8}$$

These equations are used to estimate the battery's internal temperature profile, assess heat dissipation, optimize the thermal management system, and prevent critical scenarios such as overheating or short-circuit events. The ρ, C_p, T, k, σ_+, ϕ_+, σ_-, ϕ_-, $\dot{q}_{Ech}$, $\dot{q}_{short}$, and $\dot{q}_{abuse}$ represent, respectively, the material density, specific heat, temperature, thermal conductivity, electrical conductivity, potential of the positive and negative electrodes, heat generated through electrochemical reactions, internal short circuits, and abnormal operating conditions such as overcharging or elevated temperatures. j_{Ech} and j_{short} represent the current density due to electrochemical reactions and short circuits, respectively. Equations (7) and (8) describe the current flow in the electrodes and illustrate how electrical current is distributed through conductivity and electrochemical reactions. The nonlinear governing equations were solved numerically, yielding the temperature distribution across the battery domain. The SENEC.Home V3 Hybrid 5 battery selected for this project is a lithium-ion NMC type, consisting of 14 cells rated at 94 Ah and 3.7 V, connected in series to form the complete battery pack. Figure 6 shows a single 94 Ah, 3.7 V cell.

2.6.2. Numerical Method

The thermal behavior of the lithium-ion batteries, derived from HOMER Pro data, was analyzed using simulation software to evaluate their operational safety under continuous 24-hour conditions. Each SENEC.The Home V3 Hybrid 5 battery consists of 14 cells (94 Ah, 3.7 V) connected in series, forming a 94 Ah battery with a 51.5 V voltage. In the physical

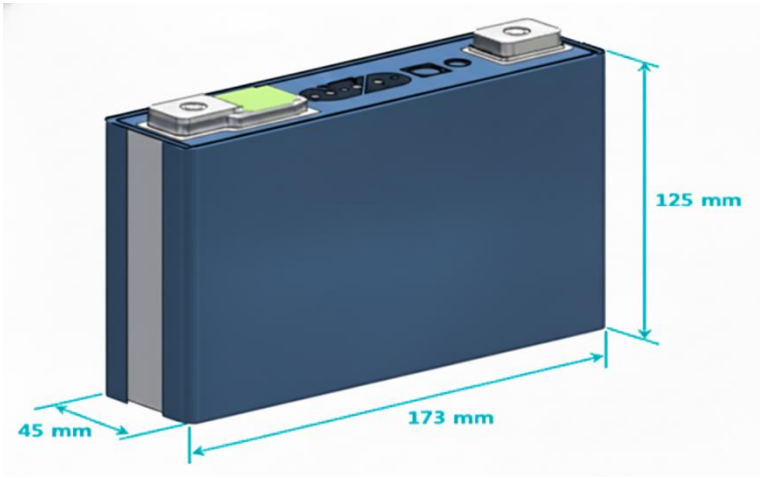

Fig. 6. The 94 Ah, 3.7 V cell.

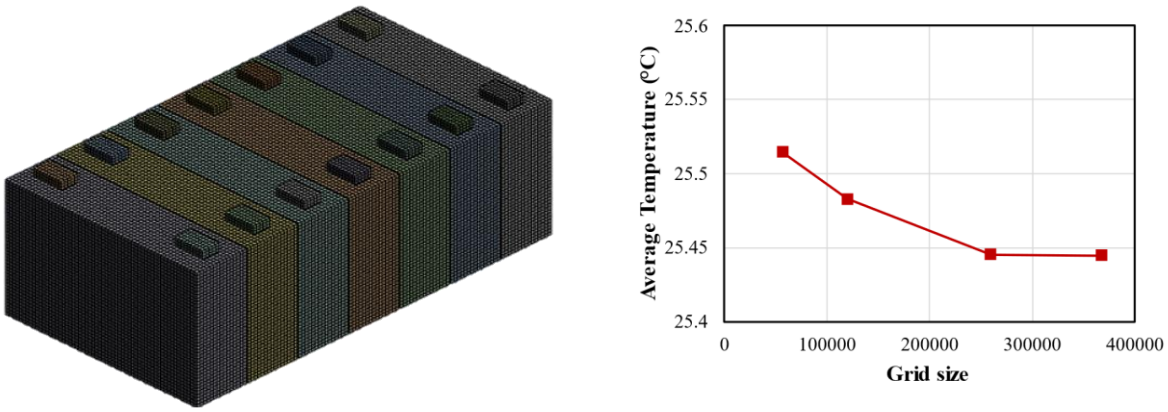

(a) (b)

Fig. 7. (a) Meshed geometry of the battery cells from ANSYS Fluent, (b) Mesh independence study of the battery cells.

configuration, the cells were arranged as seven adjacent pairs. Since temperature distribution is expected to be symmetrical across the cell pairs, thermal analysis was conducted on seven representative series-connected cells. The meshed geometry of these cells contained 258,804 elements, as shown in Fig. 7.

After generating the mesh for the battery geometry, the meshed domain was imported into ANSYS Fluent, where the thermal simulation setup was defined. A transient solution mode was selected, with the energy equation activated and the flow equations deactivated, since no fluid motion occurs inside the battery during thermal analysis. The MSMD battery model was then initialized to simulate the electrochemical-thermal coupling behavior of the cells. The Newman-Tiedemann-Gu-Kim (NTGK) model, a semi-empirical approach, was selected for the thermal simulation of the lithium-ion battery because it provides an effective balance between physical accuracy and computational efficiency for low-C-rate stationary storage applications. NTGK captures the dominant heat-generation mechanisms of ohmic, reaction, and polarization losses without the complexity of full electrochemical models, making it suitable for systems operating under mild thermal and electrical conditions. However, this model does not explicitly incorporate long-term degradation phenomena

such as Solid Electrolyte Interphase (SEI) growth, capacity fade, or mechanical aging. These limitations are acceptable for the present study, given the low C-rate and moderate temperature variations of the designed system.

The active and inactive regions of the battery corresponding to the cell layers and the tabs with busbars were defined, and the positive and negative tabs were specified. The initial state of charge (SOC) was set to 100%, representing a fully charged battery at the start of the simulation. After defining the thermal parameters and electrical connections, the material properties for the cell, electrode, and busbar regions were assigned. All thermophysical properties were assumed to be temperature-independent, and their values are listed in Table 5.

In the material definition step, the UDS diffusivity values for the positive and negative electrical potentials in the battery cell region were set to 1.19×10^6 and 9.83×10^5, respectively, corresponding to typical parameters for NMC-type lithium-ion cells. For the positive and negative tabs, the USER-DEFINED option was selected under the UDS diffusivity settings, and the msmdbatt mode was enabled to account for electrochemical reactions within the cell. After defining the material properties, each battery component was assigned its corresponding material in the Cell Zone Conditions panel.

For the boundary conditions, convective heat transfer was applied to all external surfaces, including the cell walls, positive and negative tabs, and busbars, using a heat transfer coefficient of 5 W/(m²•K). This value represents natural convection under indoor laboratory conditions, assuming the battery pack operates in a still-air environment. The surrounding air was considered quiescent and maintained at the laboratory temperature (298 K), ensuring negligible temperature gradients around the cell. Radiative heat transfer was not included in the model due to the stable ambient temperature and minimal air movement; however, radiation could become relevant in high-temperature environments or systems with larger heat sources.

A full three-dimensional model of the cell was simulated without symmetry reductions. The Second Order Upwind scheme was applied to solve the energy and electric potential equations. The simulation was manually initialized at 298 K. A time step of 1 s was chosen, and the model was run for 86,400 time steps to simulate 24 hours of continuous operation, during which the battery underwent 13 hours of discharge and 11 hours of charging.

In this study, the temperature distribution and thermal behavior of the lithium-ion NMC battery were analyzed using ANSYS Fluent. The simulation focused on evaluating the spatial temperature gradients, maximum temperature rise, and thermal uniformity within the battery cell during charge and discharge cycles. These parameters are critical for assessing the thermal stability, efficiency, and operational safety of the battery during continuous operation in the solar-powered hybrid HDH-RO desalination system. The obtained temperature contours provide valuable insight into the heat accumulation patterns and highlight the importance of effective thermal management to prevent performance degradation and extend battery lifespan.

2.7. Validation of Simulation Results

The numerical results obtained in this study were validated through comparison with previously published data, demonstrating good agreement and confirming the accuracy of the proposed approach.

Table 5. Material properties selected for the battery in Fluent.

Material	$\rho\ (\frac{kg}{m^3})$	$C_p\ (\frac{J}{kg.K})$	$k\ (\frac{W}{m.K})$
Cell material	2055	900	18
Copper (negative tab-busbar)	8978	381	387.6
Aluminum (positive tab)	2719	871	202.4

2.7.1. Validation of HOMER Pro Simulation

To verify the accuracy of the developed HOMER Pro model, the simulation results of this study were compared with those reported by Bouseba et al. [34], who analyzed a grid-connected photovoltaic system for a medium-sized building. Although the scale and application of their system (360 kW PV array and 300 kW converter) differ substantially from the small-scale, off-grid PV-battery desalination unit examined in this work (7.5 kW PV array and 1.68 kW converter), both studies employ a similar simulation framework and modeling methodology in HOMER Pro. Therefore, this comparison was performed to validate the simulation procedure and the correctness of the software implementation rather than to compare systems of equivalent capacity. In HOMER Pro, both building and desalination demands are represented as electrical load profiles; therefore, this validation primarily confirms the correctness of the PV-battery system configuration, dispatch strategy, and economic computations rather than an application-specific performance match.

The validation focused on key techno-economic performance indicators, including the Net Present Cost (NPC) and the Cost of Energy (COE). As shown in Table 6, the differences between the two studies were 1.23% for NPC and 2.46% for COE, demonstrating the reliability and accuracy of the HOMER-based modeling approach adopted in this work. The small deviations primarily result from differences in system scale, input assumptions, and local economic conditions.

2.7.2. Validation of the Thermal Battery Model

To ensure the accuracy of the thermal simulation of the lithium-ion battery pack, the numerical model was validated against the experimental data reported by Kim et al. [59], who investigated the thermal behavior of a 14.6 Ah lithium-ion cell under charge-discharge cycling. The cell was modeled and meshed in ANSYS Fluent using the same geometric dimensions, material properties, and boundary conditions as those used in the reference study. A close agreement was observed between the simulated and experimental temperature profiles, confirming that the applied boundary conditions and thermal parameters were appropriately defined. The validation results are illustrated in Fig. 8.

The primary objective of this validation was to ensure the correct implementation of the numerical framework in ANSYS Fluent for the present battery thermal analysis. This included accurate specification of material properties, proper application of boundary and contact conditions, selection of appropriate physics models, mesh quality and grid-independence checks, pressure-velocity coupling using the SIMPLE algorithm, application of second-order schemes for the energy and electric potential equations, and the selection of suitable time-step and convergence criteria within the low C-rate operating range considered in this study.

For an ambient temperature of 298K, the maximum deviation between the two curves is 2.5 % at the 4th minute of the simulation. Given this small error value, it can be concluded that the validation was successful. Moreover, the curve indicates that during the last minute of discharge, between the 10th and 11th minutes, the slope of the curve at 298K increases. The main reason for the increase in slope at the end of discharge is the rise in the battery's internal resistance due to severe discharge at a 5C rate. This increased resistance causes a larger voltage drop and sudden heat generation at the end of discharge, resulting in a temperature rise.

Table 6. Comparison between the results of Bouseba et al. (34) and the validation results.

Case	PV Array (kW)	Battery	Grid (kW)	Converter (kW)	Total Net Present Cost ($)	Cost of Energy ($/kWh)
Bouseba et al. (34)	360	-	999999	300	748413	0.0894
Validation Results	365	-	999999	300	757624	0.0916
Error (%)	1.38	-	-	0	1.23	2.46

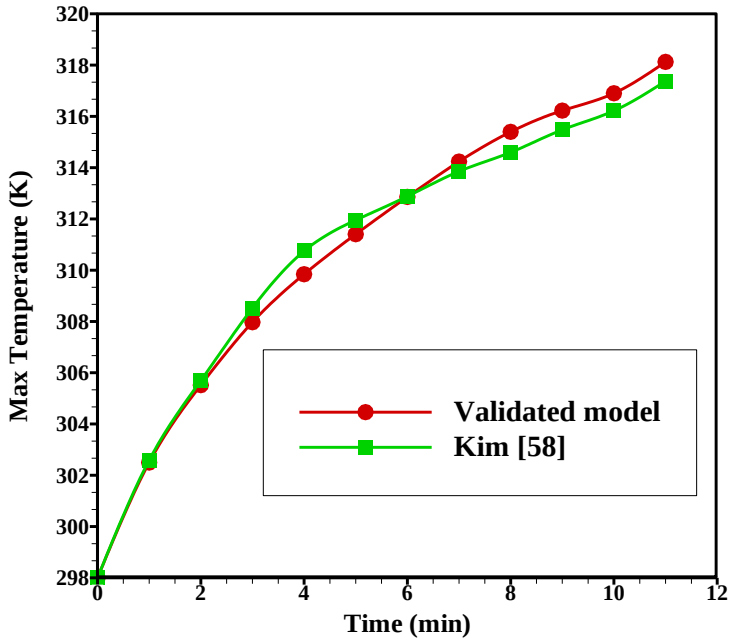

Fig. 8. Maximum battery temperature profile obtained at an ambient temperature of 298K under a discharge rate of 5C.

Overall, the validation results, including both the HOMER Pro simulations and the numerical thermal model of the battery pack, demonstrate good agreement with literature references, confirming the reliability and accuracy of the applied modeling approaches.

3. Results and discussion

In this section, the designed configuration of the power supply system for the hybrid humidification-dehumidification and reverse osmosis desalination unit is introduced and analyzed. According to the proposed structure, the system comprises solar panels and batteries that operate in two modes. Daily operation using solar energy (from 7:00 AM to 6:00 PM), during which the batteries are also charged. Nighttime operation using the batteries (from 6:00 PM to 7:00 AM), to ensure continuous freshwater production throughout the day and night. This division allows for a detailed assessment of the role of energy storage in enhancing system reliability and operational stability.

3.1. Component Configuration of the Present Study

In this study, a hybrid energy configuration consisting of solar panels and battery storage was designed to supply the power required to operate the hybrid humidification-dehumidification and reverse osmosis desalination unit. During daylight hours (7:00 AM to 6:00 PM), the desalination system's electrical demand is fully met by the photovoltaic array, while the batteries are simultaneously charged. During nighttime hours (6:00 PM to 7:00 AM), the battery bank's stored energy supplies the load, ensuring continuous 24-hour freshwater production.

In addition to the proposed solar-battery system, a diesel-only configuration was also modeled in HOMER Pro as a reference case to assess the techno-economic and environmental benefits of the renewable system. This baseline scenario assumes a standalone diesel generator operating continuously for 24 hours to meet the power demand of the hybrid HDH-RO desalination unit, enabling a direct comparison between the two energy supply strategies. The developed configurations implemented in HOMER Pro (v3.18.3) are illustrated in Fig. 9.

3.2. HOMER Pro Simulation Results

The results of the simulation and optimization of the different energy-system

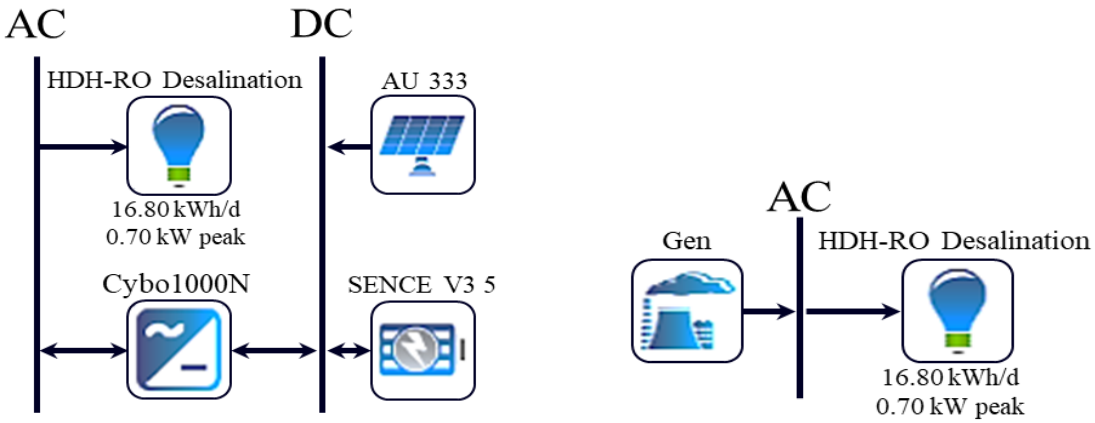

(a) (b)

Fig. 9. (a) Solar system with the hybrid humidification-dehumidification and reverse osmosis desalination unit, (b) diesel-only system from HOMER Pro.

configurations evaluated for powering the HDH-RO desalination unit are presented in this section.The economic analysis assumes a 20-year project lifetime, with a nominal interest rate of 23% and an inflation rate of 22.2%. Since economic indicators in Iran may vary over time due to market conditions and policy adjustments, representative values are commonly used in techno-economic studies to ensure consistency in long-term assessments. Accordingly, the selected rates provide realistic estimates for evaluating the economic performance of renewable-energy systems under local conditions. Several configurations were analyzed in HOMER Pro, including a standalone diesel-generator system and a separate solar-battery hybrid system for comparative evaluation.

The optimal sizing of the system components, such as photovoltaic panels, battery storage units, and the diesel generator, along with configuration details, performance indicators, and cost parameters, was determined. For each configuration, an appropriate energy management strategy covering battery charging, generator operation, and load supply during day and night was implemented to minimize costs and maximize energy efficiency. This comprehensive evaluation ensures continuous freshwater production while providing a clear techno-economic comparison between fossil-fuel-based and renewable-powered operating modes.

3.2.1. Technical Performance Results

PV-Battery-System

After entering all input parameters into HOMER Pro, the results presented in Fig. 10 were obtained. According to the HOMER Pro simulation outcomes (Fig.12), a total photovoltaic capacity of 7.5 kW was required to power the hybrid humidification-dehumidification and reverse osmosis desalination system. To achieve this capacity, 333 W nominal solar panels were used, and the required number was calculated to be 23 panels. The panels were arranged in a parallel configuration to maintain a stable system voltage and enhance the overall current flow, enabling safe battery charging at 51.5 V. Figure 11 illustrates the yearly power generation profile of the photovoltaic array.

According to Fig.11, the photovoltaic panels generate electricity between 7:00 AM and 6:00 PM, with output decreasing during the colder months. The system's peak electrical generation capacity is 7.42 kW. Since the system operates solely on solar energy, it produces no harmful emissions, including carbon dioxide, carbon monoxide, nitrogen oxides, or sulfur dioxide. Figure 12 presents the monthly variation in the photovoltaic power generation. As shown, the highest electricity production occurs during August and September. This increase is primarily due to higher solar irradiance and favorable temperature conditions during these months, both of which directly affect the panels' efficiency.

Architecture				Cost				System	
AU 333 (kW)	SENEC V3 5 (#)	Cybo1000N (kW)	NPC ($)	LCOE ($/kWh)	Operating cost ($/yr)	CAPEX ($)	Ren Frac (%)	Total Fuel (L/yr)
7.50	8	1.68	$22,576	$0.197	$223.27	$18,404	100	0
7.51	8	1.66	$22,579	$0.197	$223.23	$18,407	100	0
7.52	8	1.68	$22,586	$0.197	$223.38	$18,411	100	0
7.53	8	1.73	$22,611	$0.197	$223.81	$18,428	100	0
7.57	8	1.64	$22,618	$0.197	$223.50	$18,441	100	0
7.59	8	1.60	$22,627	$0.198	$223.42	$18,452	100	0
7.57	8	1.69	$22,629	$0.198	$223.78	$18,446	100	0
7.59	8	1.70	$22,649	$0.198	$224.00	$18,463	100	0
7.61	8	1.66	$22,650	$0.198	$223.86	$18,466	100	0
7.61	8	1.68	$22,659	$0.198	$224.02	$18,473	100	0

Fig. 10. The technical results obtained from HOMER Pro.

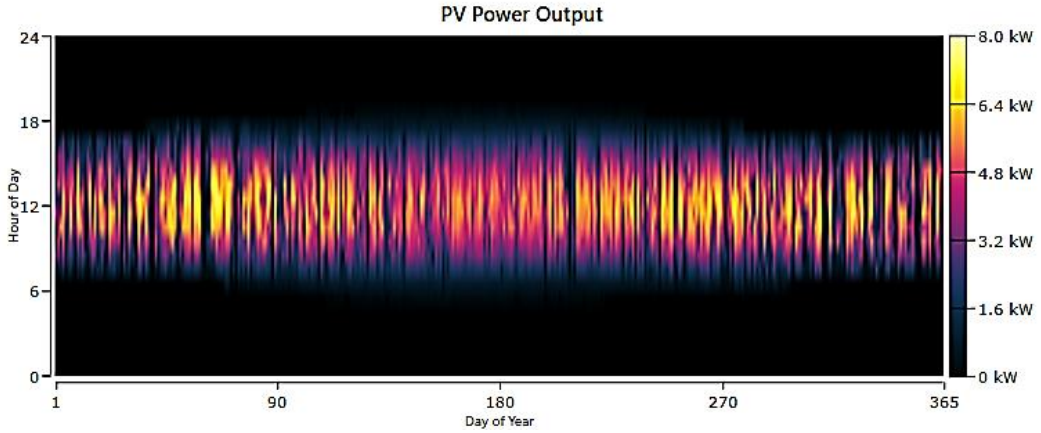

Fig. 11. Annual power output of the solar panels from HOMER Pro.

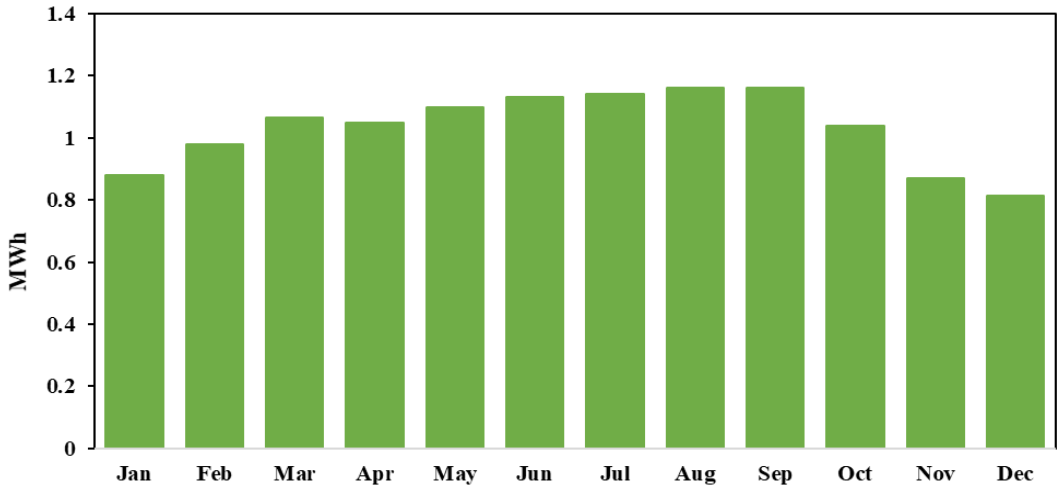

Fig. 12. Monthly power output of the solar panels from HOMER Pro.

The results indicate that the solar panels operate for 4,387 hours annually, generating a total of 12,442 kWh of electricity. After meeting the desalination unit's energy demand, approximately 5,987 kWh of surplus electricity remains each year, which can be exported to the grid for effective use.

In this study, lithium-ion NMC batteries with a nominal capacity of 94 Ah and a 51.5 V voltage rating were selected for their cost-effectiveness and suitability for solar-based applications. The required 94 Ah capacity was determined from the HOMER Pro optimization results, which indicated that eight battery modules connected in parallel were necessary to minimize the overall system cost. During daylight hours, the batteries are charged using the electricity generated by the photovoltaic panels, and at night they discharge to power the desalination unit, ensuring continuous 24-hour operation of the hybrid humidification-dehumidification and reverse osmosis system.

Under cloudy conditions, the batteries can supply energy for up to 49.8 hours without recharging. According to the simulation results, approximately 3,528 kWh of energy is stored and discharged annually (Fig.13). As illustrated in Fig.13, the batteries are charged during the day and discharged at night to meet the system's energy demand. Figure 14 shows the monthly variation in the battery state of charge. As expected, the state of charge is lower during the colder months due to reduced solar irradiance and lower photovoltaic power generation.

The simulation also demonstrated that a 1.68 kW converter can convert the outputs from both the solar panels and the battery bank into the alternating current required by the desalination unit. This converter operates for 8,757 hours per year, remaining active nearly continuously and enabling uninterrupted 24-hour operation of the system.

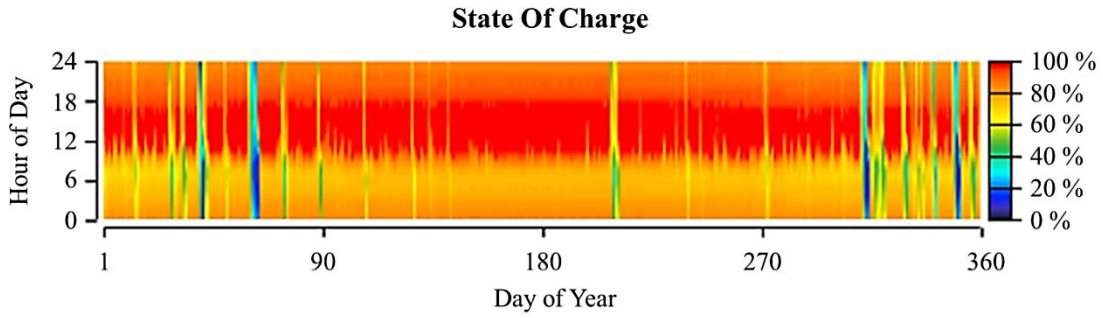

Fig. 13. Annual battery state of charge from HOMER Pro.

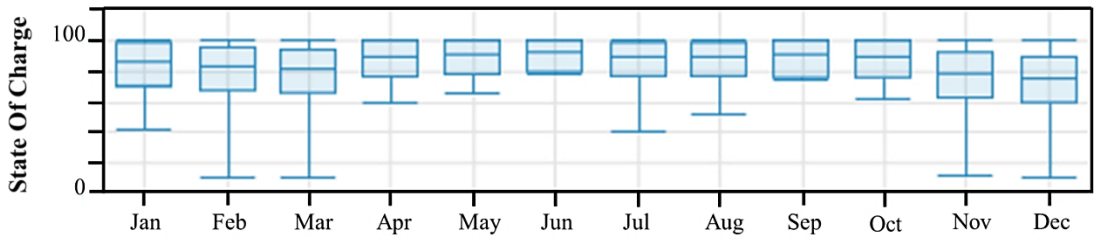

Fig. 14. Monthly state of charge of the batteries from HOMER Pro.

DG-System

According to the HOMER Pro simulation results, the diesel-only configuration was designed with a generator capacity of 0.77 kW to continuously supply the electrical demand of the hybrid HDH-RO desalination unit. The generator produces a total of 6,132 kWh of electricity annually, all derived from fossil fuels, resulting in a renewable energy fraction of 0%. The system's annual fuel consumption is 1,824 liters. Figure 15 illustrates the technical performance of the diesel-based configuration obtained from HOMER Pro.

Figure 16 presents the monthly electricity generation profile of the diesel generator (HOMER Pro v3.18.3). As shown, the generator maintains a nearly constant power output throughout the year, producing approximately 0.5 MWh per month to continuously supply the 700 W load of the hybrid HDH-RO desalination unit. The slight variations observed between months are attributed to minor fluctuations in system efficiency and fuel consumption during long-term operation. Since the generator provides the entire energy demand, the system operates with no renewable contribution.

Table 7 presents the estimated air pollutant emissions from the diesel generator during operation, including carbon dioxide (CO_2), carbon monoxide (CO), nitrogen oxides (NO_x), and sulfur dioxide (SO_2). These emissions were automatically calculated by HOMER Pro based on the generator's fuel consumption rate and performance characteristics, highlighting the substantial environmental burden of the fossil-fuel-based configuration compared to the zero-emission solar-battery system.

The environmental assessment of the diesel-only configuration indicates significant pollutant emissions resulting from continuous fossil fuel combustion. As shown in Table 7, the diesel generator produces 4,775 kg of CO_2, 30.1 kg of CO, 1.31 kg of unburned hydrocarbons, 11.7 kg of SO_2, and 28.3 kg of NO_x annually. These pollutants contribute not only to greenhouse gas accumulation and climate change but also to local air-quality degradation through the release of toxic and acid-forming compounds. In contrast, the proposed solar-battery hybrid system produces zero direct emissions, as the entire energy demand of the desalination unit is met by photovoltaic generation and battery storage.

Architecture	Cost				System		Project Economics		Gen				
Gen (kW)	NPC ($)	LCOE ($/kWh)	Operating cost ($/yr)	CAPEX ($)	Ren Frac (%)	Total Fuel (L/yr)	IRR (%)	Simple Payback (yr)	Hours	Production (kWh)	Fuel (L)	O&M Cost ($/yr)	Fuel Cost ($/yr)
0.770	$30,651	$0.267	$1,544	$1,798	0	1,824			8,760	6,132	1,824	202	1,094

Fig. 15. The techno-economic performance results of the diesel-generator-based system obtained from HOMER Pro.

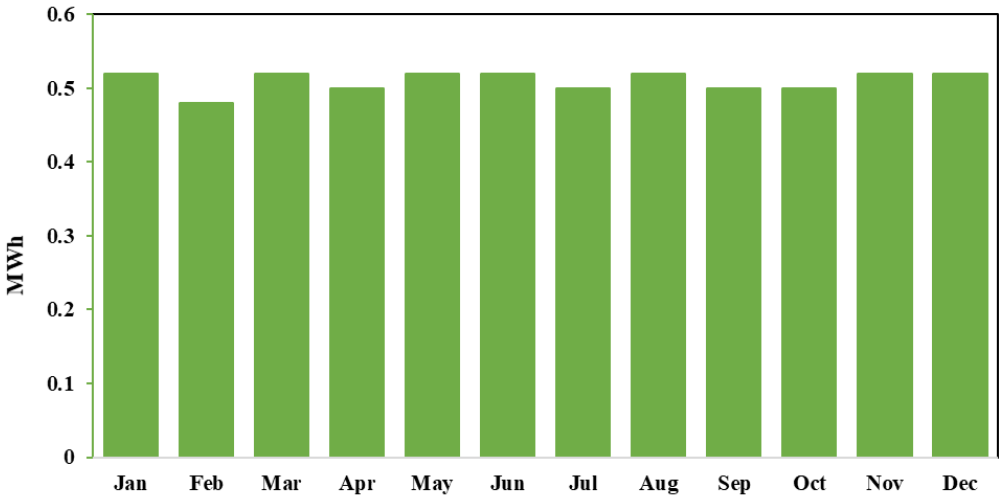

Fig. 16. Monthly electricity generation profile of the diesel generator obtained from HOMER Pro.

Table 7. air pollutants emitted by the diesel generator.

Content	Emission rate
Carbon Dioxide	4775 kg/yr
Carbon Monoxide	30.1 kg/yr
Unburned Hydrocarbons	1.31 kg/yr
Sulfur Dioxide	11.7 kg/yr
Nitrogen Oxides	28.3 kg/yr

3.2.2. Economic Performance Results

PV-Battery-System

This section presents the economic evaluation based on the results generated using HOMER Pro. As described in Section 2.4, HOMER Pro identifies the configuration that satisfies the project's technical requirements while minimizing the overall cost. According to the optimization results (Fig. 10), the Net Present Cost (NPC) of the system is estimated at $22,576, with a Levelized Cost of Energy (LCOE) of $0.197/kWh. The annual operating cost is $223.27, while the initial capital expenditure (CAPEX) is $18,404. Figure 17 illustrates the cost distribution among the system components. Since the desalination-unit costs cannot be directly incorporated into HOMER, we calculated the NPC of the desalination unit manually using Eqs. (1) and (2). In this calculation, the desalination unit capital cost, O&M cost, and 20-year lifetime were considered, and the system real discount rate computed by HOMER (0.65%) was used. Accordingly, the NPC of the desalination unit was obtained as $3,370. This value was then added to the NPC of the energy-supply system obtained from HOMER, resulting in a total system NPC of $25,946.

As shown in Fig. 17, the largest cost contribution is from lithium-ion batteries. Despite their higher cost relative to other battery technologies, their long lifespan and high efficiency in renewable energy systems make them an appropriate choice for this 20-year project. The component costs are as follows: batteries $13,495; solar panels $5,729; installation and maintenance $2,402; charge controller $787.5; and converter $404.5. Additionally, the residual cost for decommissioning the solar panels at the end of their service life is $839.3. Figure 18 presents the project cash flow over the 20 years.

The hybrid humidification-dehumidification and reverse osmosis desalination unit produces 3.72 m³ of freshwater per day, resulting in a total production of 27,156 m³ over the 20-year project lifetime. Given the total project cost of $25,946, the cost of producing one cubic meter of freshwater, calculated using Eq. (5), is $0.95/m³.

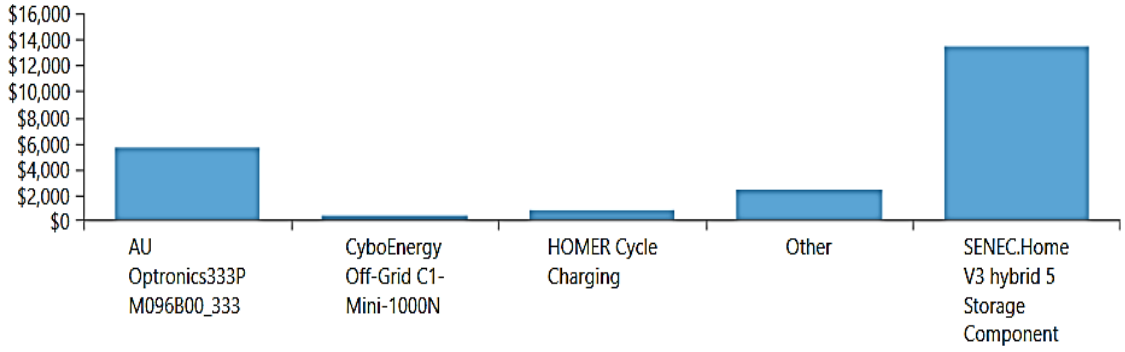

Fig. 17. The Cost distribution for the PV-Battery-System in the project from HOMER Pro.

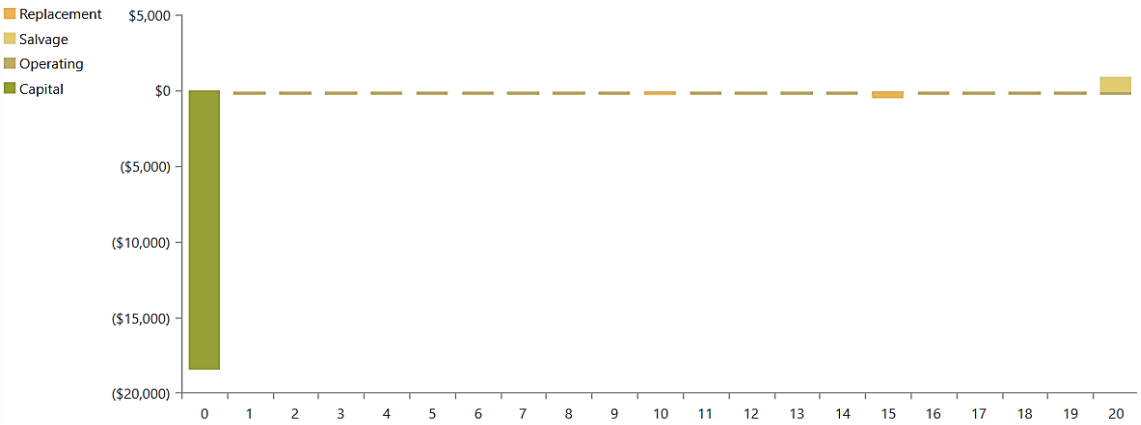

Fig. 18. The project cash flow diagram over the 20 years from HOMER Pro for the PV-Battery-System.

DG-System

This section presents the economic evaluation of the diesel-only configuration based on HOMER Pro results. Similar to the hybrid renewable analysis, HOMER Pro identified the optimal operating parameters that minimize the overall system cost while meeting the desalination unit's continuous power demand. As shown in Fig.15, the Net Present Cost (NPC) of the diesel-based system is $30,651, with a Levelized Cost of Energy (LCOE) of $0.267 per kilowatt-hour. By including the desalination-unit NPC, the total NPC is $34,021. The annual operating cost is estimated at $1,544, primarily due to fuel expenses amounting to $1,094 per year. The initial capital cost (CAPEX) of the diesel generator is $1,798, reflecting its relatively low upfront investment but significantly higher long-term operating expenditure.

As illustrated in Fig. 19, the economic results highlight the substantial contribution of fuel and maintenance costs to the overall project budget, thereby increasing the lifetime cost compared with the solar-battery configuration.

Figure 20 presents the annual cash flow diagram for the diesel generator-based configuration generated in HOMER Pro (v3.18.3). As shown, the system requires an initial capital investment of $1,798 at the start of the project (year 0). In subsequent years, the major expenses are associated with fuel consumption and periodic replacement costs, which recur regularly throughout the 20-year project lifetime. The annual operation and maintenance costs remain nearly constant, while fuel expenses account for the largest share of total annual expenditure. A small salvage value is recorded at the end of the project, partially offsetting the final-year costs.

The cash flow analysis clearly demonstrates that the diesel-only system is heavily dependent on recurring fuel expenses, resulting in a continuous financial burden over time. In contrast, the solar-battery system incurs higher initial capital costs but minimal operating expenses, leading to substantially lower lifetime costs and significantly improved long-term economic feasibility.

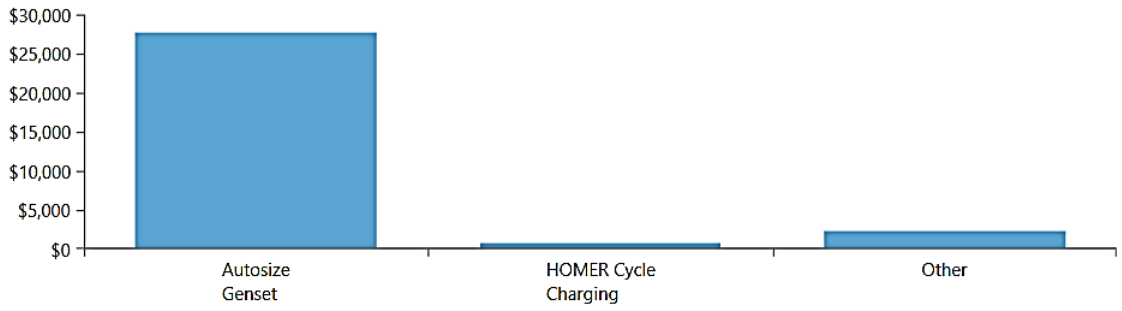

Fig. 19. The Cost distribution for the DG-System in the project from HOMER Pro.

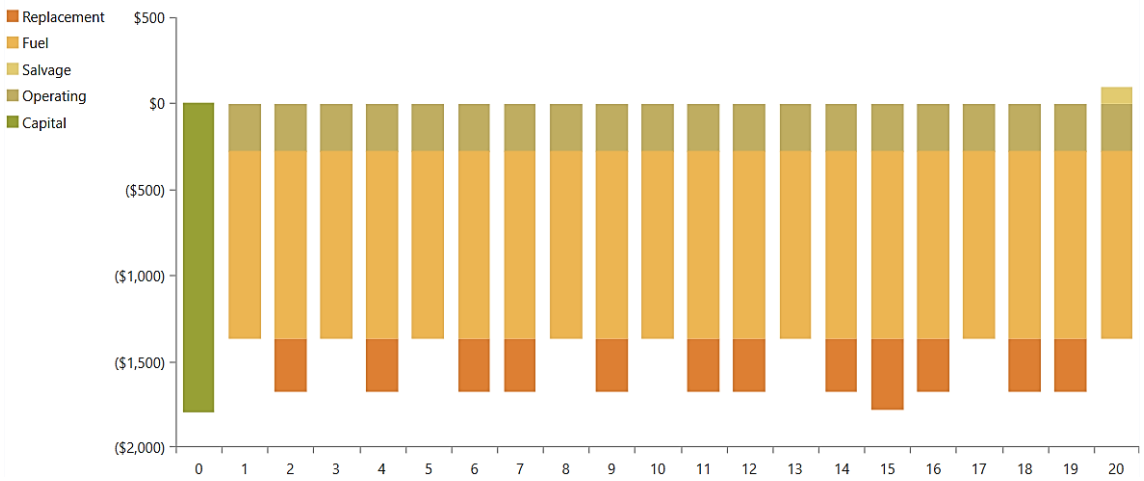

Fig. 20. The project cash flow diagram over 20 years from HOMER Pro for the DG-system.

Considering that the hybrid humidification-dehumidification and reverse osmosis desalination unit produces 3.72 m³ of freshwater per day, the total freshwater production over the 20-year project lifetime is 27,156 m³. For the diesel-only configuration, the total Net Present Cost (NPC) is $34,021. Using Eq.(5), the corresponding Levelized Cost of Water (LCOW) is calculated as $1.25/m³. This value is substantially higher than the LCOW of the proposed solar-battery system ($0.95/m³), indicating that the renewable configuration achieves a 24% reduction in freshwater production cost compared to the diesel-based alternative.

These findings clearly demonstrate the superior economic and environmental performance of the solar-powered hybrid HDH-RO desalination system, underscoring its strong potential as a sustainable, cost-effective solution for off-grid freshwater production.

Figure 21 compares the cumulative cash flows of the proposed solar-battery-powered desalination system and the diesel-based reference system over the 20-year project lifetime. As shown, the cumulative cash flow curves of the two configurations reveal a clear difference in their long-term economic performance. The diesel-based system experiences a continuous decline in cumulative cash flow throughout the project duration due to persistent fuel and maintenance expenses, and it never achieves cost recovery.

In contrast, the proposed solar-battery system shows gradual improvement in its cumulative balance, reaching breakeven after 13 years of operation. Beyond this point, the system begins to generate a net economic benefit, attributed to its minimal operating costs and complete independence from fuel consumption. These results confirm that, despite requiring a higher initial investment, the renewable configuration offers a significantly shorter payback period and greater long-term profitability compared to the diesel-only system.

Based on the comprehensive techno-economic and environmental analyses conducted in this study, the solar-battery-powered hybrid desalination system is identified as the optimal configuration among the evaluated scenarios. The HOMER Pro optimization results show that this system achieves the lowest Net Present Cost (NPC) and Levelized Cost of Water (LCOW) while ensuring uninterrupted 24-hour operation without reliance on fossil fuels. In contrast, although the diesel-based system can provide stable power, it incurs significantly higher operating expenses and substantial pollutant emissions.

Therefore, the proposed renewable configuration not only offers superior economic feasibility through reduced lifetime costs and a 13-year payback period but also enhances environmental sustainability by eliminating fuel consumption and greenhouse gas emissions. Consequently, the solar-battery hybrid system represents the most efficient and sustainable design option for off-grid freshwater production using the combined HDH-RO desalination process.

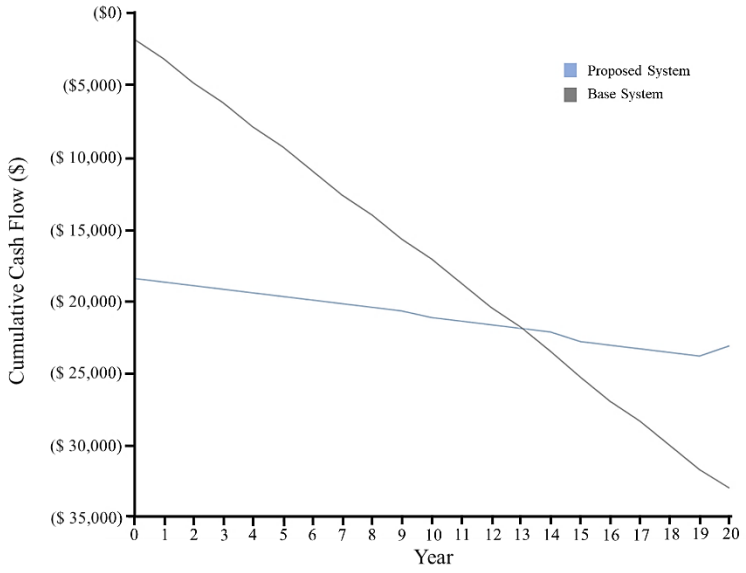

Fig. 21. Cumulative cash flow curves of the proposed solar-battery system and the diesel-only reference system.

3.2.3. Sensitivity Analysis

To assess the stability and reliability of the simulation results, a sensitivity analysis was conducted in HOMER Pro to examine variations in solar irradiance. Since solar radiation is the primary energy source for this system, fluctuations in irradiance can significantly influence power generation capacity and, consequently, the performance of the combined humidification-dehumidification and reverse osmosis desalination unit. For this purpose, different annual solar irradiance values were input into the model, and the resulting total system cost and energy production cost were evaluated. The outcomes of this analysis are presented in Fig.22.

As shown in Fig. 22, an increase in solar irradiance reduces both the Net Present Cost (NPC) and the cost of energy generation. This reduction is mainly due to the lower number of batteries required as solar irradiance levels rise. Therefore, implementing the proposed system in off-grid tropical and arid regions with considerably higher annual solar radiation levels can substantially reduce overall system costs and freshwater production expenses, making the configuration particularly suitable for remote areas.

Lithium-ion batteries represent the primary capital cost in the proposed solar-powered hybrid HDH-RO desalination system. Considering the ongoing global trend of declining lithium-ion battery prices driven by increased production capacity and technological advancements, the overall system cost is expected to decrease significantly in the future. As battery prices fall, both the NPC and the system's Cost of Energy (COE) will be reduced, since energy storage accounts for a major portion of total expenses. This cost reduction will be particularly advantageous for large-scale projects and remote regions that require economically sustainable solutions, ultimately enhancing both the financial and operational performance of the system.

Solar Scaled Average (kWh/m²/day)	AU 333 (kW)	SENEC V3 5 (#)	Cybo1000N (kW)	NPC ($)	LCOE ($/kWh)	Operating cost ($/yr)	CAPEX ($)	Ren Frac (%)
3.50	13.9	7	1.69	$25,743	$0.225	$256.29	$20,953	100
4.50	7.78	8	1.64	$22,776	$0.199	$224.89	$18,573	100
5.56	8.67	7	1.35	$21,696	$0.189	$219.04	$17,602	100
6.00	8.02	7	1.33	$21,199	$0.185	$214.58	$17,189	100
7.50	6.39	7	0.880	$19,848	$0.173	$200.79	$16,096	100

Fig. 22. The results of the HOMER Pro sensitivity analysis.

In Fig. 23, obtained from the HOMER software, presents the sensitivity analysis of the hybrid energy system with lithium-ion batteries. This analysis evaluates the effects of variations in the Initial State of Charge (SOC) and Minimum State of Charge on several system performance metrics. The initial SOC values range from 60% to 90%, while the minimum SOC values range from 5% to 40%.

The results show that increasing the initial SOC reduces the Net Present Cost (NPC) but increases operational costs. Although NPC experiences only minor changes, the Levelized Cost of Energy (LCOE) increases as the initial SOC rises from 60% to 80%. Increasing the minimum SOC from 10% to 40% generally results in higher NPC and LCOE. Operational costs also increase with higher minimum SOC values. While CAPEX is not directly affected, variations in battery capacity can lead to a higher initial investment.

In general, lithium-ion batteries are commonly operated within an SOC window of about 10% to 80%, as this range provides a practical compromise between cost, usable capacity, and cycle life. In other words, this SOC window is often considered an overall optimal operating range for Li-ion batteries in real applications. However, if the objective is to prioritize battery lifetime alone (with less emphasis on maximizing usable capacity), a narrower SOC window, such as 40% to 70%, can be more suitable. This recommendation is also supported by Li et al. [61].

3.3. Thermal Analysis Result

3.3.1. Coupling Procedure Between HOMER Pro Outputs and the MSMD/NTGK Battery Thermal Model

The thermal analysis in this study is directly linked to the techno-economic sizing and dispatch results obtained from HOMER Pro. Specifically, HOMER Pro determines (i) the required number of batteries to ensure continuous (24-h) operation of the hybrid HDH-RO desalination system, and (ii) the corresponding charging/discharging electrical conditions that are subsequently applied in the battery thermal model.

Based on the HOMER Pro optimal configuration, continuous operation of the desalination unit requires eight [8] Li-ion NMC batteries, each with a nominal capacity of 94 Ah and a nominal voltage of 51.5 V, connected in parallel. Each NMC battery pack consists of 14 cells (94 Ah, 3.7 V) connected in series, yielding the stated pack voltage.

Sensitivity		Architecture					Cost			
Initial State Of Charge (%)	Minimum State Of Charge (%)				AU 333 (kW)	SENEC V3 5 (#)	Cybo1000N (kW)	NPC ($)	LCOE ($/kWh)	Operating cost ($/yr)	CAPEX ($)
60.0	10.0				7.50	8	1.68	$22,576	$0.197	$223.27	$18,404
60.0	20.0				7.50	9	1.70	$24,263	$0.212	$233.35	$19,902
60.0	30.0				12.7	8	1.75	$26,595	$0.232	$259.14	$21,751
60.0	40.0				11.3	10	1.17	$28,707	$0.251	$265.59	$23,744
60.0	5.00				9.03	7	1.87	$22,099	$0.193	$224.76	$17,898
70.0	10.0				7.50	8	1.68	$22,576	$0.197	$223.27	$18,404
70.0	20.0				7.50	9	1.70	$24,263	$0.212	$233.35	$19,902
70.0	30.0				12.7	8	1.75	$26,595	$0.232	$259.14	$21,751
70.0	40.0				11.3	10	1.17	$28,707	$0.251	$265.59	$23,744
70.0	5.00				9.03	7	1.87	$22,099	$0.193	$224.76	$17,898
80.0	10.0				7.50	8	1.68	$22,576	$0.197	$223.27	$18,404
80.0	20.0				7.50	9	1.70	$24,263	$0.212	$233.35	$19,902
80.0	30.0				12.7	8	1.75	$26,595	$0.232	$259.14	$21,751
80.0	40.0				11.3	10	1.17	$28,707	$0.251	$265.59	$23,744
80.0	5.00				9.03	7	1.87	$22,099	$0.193	$224.76	$17,898
90.0	10.0				7.50	8	1.68	$22,576	$0.197	$223.27	$18,404
90.0	20.0				7.50	9	1.70	$24,263	$0.212	$233.35	$19,902
90.0	30.0				12.7	8	1.75	$26,595	$0.232	$259.14	$21,751
90.0	40.0				11.3	10	1.17	$28,707	$0.251	$265.59	$23,744
90.0	5.00				9.03	7	1.87	$22,099	$0.193	$224.76	$17,898

Fig. 23. Sensitivity analysis of the hybrid energy system showing the impact of varying the Initial and Minimum State of Charge on system performance.

The combined HDH–RO unit requires 700 W of electrical power. Accordingly, the required electrical current for supplying the desalination load is 14.6 A (depending on the operating voltage level). Since the battery packs are connected in parallel (8 strings), the discharge current is shared among them, resulting in an average discharge current of approximately 1.8 A per battery pack. Because the cells within each pack are connected in series, the cell current equals the pack current, i.e., each cell also experiences approximately 1.8 A during discharge. Under the nominal capacity of 94 Ah, this discharge current corresponds to a mild operating condition of about 0.02C.

According to the HOMER Pro operation schedule, the batteries supply the load for approximately 13 hours per day (nighttime operation). Therefore, in the MSMD battery model, the discharge stage was implemented as 13 h at 0.02C.

For the charging stage, the PV output current varies throughout the day with solar irradiance. To represent this behavior in a simplified but practical manner for thermal simulation, an average PV charging current was adopted. Based on the PV output level in HOMER Pro, an average charging current of 3.5 A was applied, which corresponds to approximately 0.04C for a 94 Ah battery. Accordingly, the charging stage was implemented in the MSMD battery model as 11 h at 0.04C.

In summary, the HOMER-derived electrical inputs (parallel battery count, discharge/charge durations, and the corresponding pack-level operating C-rates) were used as the operating conditions for the MSMD/NTGK-based thermal simulation to evaluate the battery temperature evolution over a full 24-hour cycle.

3.3.2. Battery temperature contour

The thermal simulation of the battery cells was performed with a time step of 1 second over 86,400 time steps, corresponding to a 24-hour period. The resulting battery cell temperatures are shown in Fig. 24. As illustrated, the surface temperature of the battery cells increases by 6.3 K during 24 hours of operation. This slight temperature rise is primarily attributed to the low charge and discharge rates of 0.04 C and 0.02 C, respectively. Under such low C-rate conditions, internal heat generation is minimal, and the long charge-discharge durations allow sufficient time for the generated heat to diffuse uniformly throughout the cell.

Previous studies using electrochemical-thermal coupled models [60] have demonstrated that the current rate (C-rate) strongly influences internal heat generation and the resulting temperature distribution. Consistent with these findings, the batteries in the present study, charged at 0.04 C for 11 hours and discharged at 0.02 C for 13 hours, exhibited a nearly uniform surface temperature profile due to low internal heat production and adequate time for thermal diffusion. As a result, the simulated temperature field displayed an almost uniform distribution, with negligible differences between hot spots and cooler regions across the battery surface.

Although the temperature rise is moderate, it can still have important implications for battery durability and overall system performance. Even a small increase in temperature within the range of 5-10 K can accelerate internal degradation mechanisms and lead to a gradual loss of capacity over time. Previous studies have shown that a 10 K increase in operating temperature can nearly double the degradation rate, thereby shortening battery lifespan and reducing overall system efficiency. Therefore, maintaining the battery temperature within a safe operational range (below 313 K) is essential to ensure long-term performance stability and to minimize replacement and maintenance costs.

Given the system's continuous operation, an effective thermal management strategy may be beneficial, particularly if the battery temperature approaches safety limits, to mitigate heat accumulation and potential thermal degradation. This analysis provides insight into the batteries' thermal behavior and operational reliability over the 24-hour cycle.

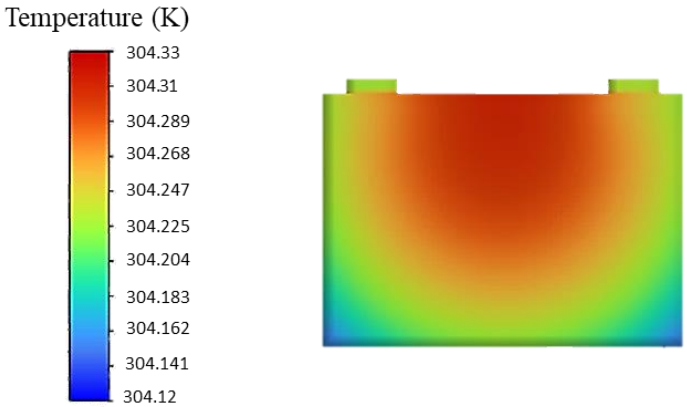

Fig. 24. Temperature contour of the battery cells over a 24-hour period obtained from ANSYS Fluent.

In this study, a 20-year lifetime is assumed for the battery based on the system's mild operating profile (Datasheet). The battery undergoes an equivalent full-cycle depth of approximately 0.4 cycles per day (157 per year), corresponding to about 3,100 cycles over 20 years. This cycling intensity falls within the commonly reported durability range for NMC batteries. Additionally, the system operates at low C-rates, and the thermal simulation results show only a 6.3 K increase in temperature, indicating that the battery remains within safe thermal limits. These conditions, taken together, reduce degradation and support the feasibility of long-term operation over the assumed lifetime.

3.4. Comparison with Previous Studies

In the previous section, the main results and performance analyses of the hybrid HDH-RO desalination system powered by photovoltaic panels and lithium-ion batteries were presented and interpreted. This section compares the obtained findings with those reported in previous studies and discusses the advantages and potential improvements of the proposed configuration. The discussion aims to highlight the novelty, practical implications, and significance of the results in the context of sustainable desalination technologies.

To validate and assess the performance of the proposed system, the obtained results were compared with those reported in previous studies. In particular, the comparison focuses on the Levelized Cost of Water and overall system efficiency to highlight the advantages of the present configuration. As summarized in Table 8, the proposed solar-battery-powered HDH-RO desalination system demonstrates a lower LCOW and improved performance compared to the literature, confirming the effectiveness of the system design.

Table 8. Results comparison with the literature.

Reference	Year	System Configuration	City, Country	LCOW ($/m^3)
Abdullah et al. (24)	2024	PV-Battery-(HDH-RO)	Saudi Arabia	0.63
Jamil et al. (50)	2018	PV-(HDH-RO)	Pakistan	0.12
Ramazanian et al. (15)	2023	PV-WT-Battery-RO	Ilam, Iran	0.9
Monnot et al. (17)	2018	PV-(with and without Battery)-RO	Kolkata, India	0.6 – 2.9
Elmaadawy et al. (18)	2020	PV-Wind-DG-Battery-RO	Abo Ramad village, Egypt	1.1 – 1.3
Current study	2025	PV-Battery-(HDH-RO)	Tehran, Iran	0.95

As shown in Table 8, the Levelized Cost of Water (LCOW) obtained in the present study ($0.95/m³) is among the lowest reported in the literature for renewable-powered desalination systems. Previous studies, such as Elmaadawy et al. [18], reported higher water production costs (1.1-1.3 $ /m³) due to the incorporation of diesel generators and partial dependence on fossil fuels. Although Ramazanian et al. [15] and Monnot et al. [17] achieved comparable costs through renewable integration, their systems were either limited in scale or operated intermittently.

In contrast, the PV-Battery-(HDH-RO) configuration proposed in this study operates entirely on clean solar energy with zero direct/operational emissions, ensuring 24-hour autonomous operation and continuous freshwater production at a substantially lower cost. Notably, studies focusing specifically on hybrid HDH-RO desalination, such as those by Abdullah et al. [24] and Jamil et al. [50] have shown that integrating energy recovery devices (e.g., pressure exchangers and Pelton turbines) and thermal enhancement techniques (such as solar preheating and coupling with heat pumps) can significantly improve energy efficiency and reduce LCOW.

Building on these advancements, the present research introduces a fully solar-powered off-grid HDH-RO system, optimized with HOMER Pro and thermally validated with ANSYS Fluent. The findings demonstrate a well-balanced combination of energy sustainability, technical performance, economic feasibility, and environmental compatibility achieved without any pollutant emissions.

Moreover, combining the renewable power supply approach developed in this study with the performance enhancement methods reported in Abdullah et al. and Jamil et al. could further enhance system efficiency, enabling higher freshwater production than the current configuration while reducing the overall water cost even further. This potential integration represents a promising direction for future research on next-generation, high-efficiency, and zero-emission desalination systems for off-grid regions.

3.5. Practical Application and Regional Significance (Case of Hengam Island)

The simulations in this study were carried out using climatic and solar radiation data for Tehran. The proposed PV-Battery-(HDH-RO) configuration shows strong potential for deployment in remote, off-grid coastal regions of southern Iran. For example, Hengam Island (26°39.2′ N, 55°52.8′ E) in Hormozgan Province is not connected to the national power grid and currently relies on diesel generators to meet its limited electricity demand. The island's existing desalination units are RO-based systems with relatively low efficiency, operating on diesel power, which leads to high fuel consumption, elevated operational costs, and considerable environmental pollution.

To address the location-dependence of the results, Hengam Island was also considered in the HOMER Pro sensitivity analysis by setting the location to Hengam and using its site-specific solar resource. In particular, a simulation was performed for an average solar irradiation of 5.56 kWh/m²/day, which corresponds to Hengam Island, and the resulting techno-economic indicators were obtained and discussed. Implementing the proposed system in such a location would replace diesel-based power generation with fully renewable solar energy, eliminating greenhouse gas and pollutant emissions while ensuring continuous freshwater production throughout the day. This clean, autonomous, and sustainable operation makes the configuration highly appropriate for environmentally sensitive and isolated regions.

Furthermore, the findings of this research provide a foundation for enhancing system efficiency, improving the quality and quantity of produced freshwater, and scaling up hybrid HDH-RO desalination systems to larger capacities. This can ultimately enable efficient, sustainable, and emission-free freshwater production for coastal and island communities in the future.

As illustrated in Fig. 12, the photovoltaic array not only meets the constant power demand of the hybrid HDH-RO desalination system but also generates 5,987 kWh of surplus electricity annually. Building on this result, the system's scalability provides an

additional practical advantage. In larger-scale implementations where desalination capacity and, consequently, the PV array and battery storage grow proportionally, the design evolves into a dual-purpose clean-energy solution.

In the specific context of Hengam Island (Hormozgan Province), where electricity generation currently depends entirely on diesel generators, this configuration achieves two objectives simultaneously: it enables continuous, 24-hour freshwater production powered exclusively by renewable energy, and it supplies excess clean electricity to the island's grid. Thus, the proposed system not only eliminates the diesel consumption previously required for operating desalination units but also partially offsets the island's diesel-based electricity generation.

This dual benefit significantly reduces greenhouse gas and pollutant emissions, decreases dependence on fossil fuels, and supports the transition toward a sustainable, zero-emission energy-water nexus for remote coastal regions.

3.6. Potential Social and Economic Impacts in Off-Grid Regions

Beyond the techno-economic and environmental advantages, the proposed solar-battery-powered hybrid HDH-RO desalination system offers substantial socio-economic benefits for off-grid and water-scarce regions. Although the estimates presented in this study correspond to a laboratory-scale desalination unit, larger-scale implementations such as those suitable for Hengam Island are expected to yield proportionally greater socio-economic and environmental gains.

Rural and island communities in southern Iran typically rely on diesel-powered RO units, which currently supply less than 30% of the local freshwater demand due to fuel shortages and high operating costs. Implementing the proposed renewable configuration could provide a continuous and autonomous freshwater supply, potentially increasing water availability by more than 200% compared to existing systems. Furthermore, in the studied off-grid case, the proposed PV-battery system not only supplies the desalination load but also generates additional electricity that can be utilized as surplus power. Specifically, the PV-battery system produces 12,442 kWh/year, of which 6,132 kWh/year is used to supply the HDH-RO desalination load, and the remaining portion is surplus electricity. For the diesel-based baseline, Table 7 reports approximately 4.9 tons/year of total pollutants for producing the 6,132 kWh/year required by the desalination load. If the diesel system is instead considered to generate the same total annual electricity as the PV-battery system (i.e., 12,442 kWh/year, including the surplus electricity), the total annual pollutants approximately double to about 9.8 tons/year. These values are obtained directly from the HOMER Pro emissions outputs under the stated assumptions. Eliminating diesel consumption of approximately 3,700 liters per year for small-scale RO units would reduce local fuel expenses by about $2,200 annually and decrease air pollutant emissions by nearly 9.8 tons per year.

These improvements can directly enhance agricultural productivity, reduce public health risks associated with limited water access, and create employment opportunities in the installation and maintenance of the system. Consequently, adopting this system supports sustainable rural development and strengthens the energy-water-food nexus in remote coastal regions of Iran.

4. Conclusions

This study demonstrated that a fully solar-powered hybrid HDH-RO desalination system supported by lithium-ion (NMC) battery storage can provide a reliable and continuous freshwater supply for off-grid regions. Through techno-economic optimization in HOMER Pro and thermal validation in ANSYS Fluent, the system was shown to operate 24 hours per day without relying on fossil fuels while maintaining safe battery temperatures, with only a 6.3 K increase during a full charge-discharge cycle.

The optimized PV-battery configuration achieved a low Levelized Cost of Water (0.95 $/m^3), outperforming conventional diesel-powered desalination systems both economically and environmentally. When applied to Hengam Island, an isolated region

with high solar irradiance, the system not only replaces diesel for desalination but also supplies surplus renewable electricity to the local grid, reducing annual air pollutant emissions by nearly 9.8 tons.

Overall, the proposed system represents a scalable, sustainable solution to water-energy challenges in remote coastal and island communities. It eliminates fuel dependency, reduces operational costs, and ensures continuous freshwater production with zero direct/operational emissions. Future work should focus on large-scale field deployment, integration with multi-renewable hybrid microgrids, and advanced control strategies to enhance long-term system resilience and performance.

Declaration of Competing Interest

There are no competing interests that could have appeared to influence the work reported in this paper.

Author Contributions

Alireza Asgharzadeh Karamshahlu: Conceptualization, Methodology, Software, Validation, Formal analysis, Investigation, Resources, Data curation, Writing original draft. **Mohammad Hassan Saidi:** Conceptualization, Supervision, Project administration, Writing review and editing. **Hooman Bahman Jahromi:** Writing original draft, Visualization, Writing review and editing. **Mohammad Behzadi Sarok:** Writing review and editing, Visualization.

References

[1] Almasoudi S, Jamoussi B. Desalination technologies and their environmental impacts: A review. Sustain Chem One World. 2024 Mar 1;1:100002.

[2] Hegazy AH, Teamah MA, Hanafy AA, El-Maghlany WM. Experimental Study of a Water Desalination System Based on Humidification-Dehumidification Process Using a Heat Pump. In: Volume 6A: Energy. American Society of Mechanical Engineers; 2015. p. V06AT07A029.

[3] Kandeal AW, Joseph A, Elsharkawy M, Elkadeem MR, Hamada MA, Khalil A, et al. Research progress on recent technologies of water harvesting from atmospheric air: A detailed review. Sustain Energy Technol Assessments. 2022 Aug;52:102000.

[4] Sun Q, Mao Y, Wu L. Research progress on the integration and optimal design of desalination process. Sep Purif Technol. 2024 Jun;337:126423.

[5] Mohamed ASA, Ahmed MS, Maghrabie HM, Shahdy AG. Desalination process using humidification–dehumidification technique: A detailed review. Int J Energy Res. 2021 Mar 10;45(3):3698–749.

[6] KALOGIROU S. Seawater desalination using renewable energy sources. Prog Energy Combust Sci. 2005;31(3):242–81.

[7] Bundschuh J, Kaczmarczyk M, Ghaffour N, Tomaszewska B. State-of-the-art of renewable energy sources used in water desalination: Present and future prospects. Desalination. 2021 Jul;508:115035.

[8] Supapo KRM, Lozano L, Tabañag IDF, Querikiol EM. A Backcasting Analysis toward a 100% Renewable Energy Transition by 2040 for Off-Grid Islands. Energies. 2022 Jun 30;15(13):4794.

[9] Al-Badi A, Al Wahaibi A, Ahshan R, Malik A. Techno-Economic Feasibility of a Solar-Wind-Fuel Cell Energy System in Duqm, Oman. Energies. 2022 Jul 25;15(15):5379.

[10] Islam M, Akter H, Howlader H, Senjyu T. Optimal Sizing and Techno-Economic Analysis of Grid-Independent Hybrid Energy System for Sustained Rural Electrification in Developing Countries: A Case Study in Bangladesh. Energies. 2022 Sep 1;15(17):6381.

[11] Cornejo-Ponce L, Vilca-Salinas P, Arenas-Herrera MJ, Moraga-Contreras C, Tapia-Caroca H, Kukulis-Martínez S. Small-Scale Solar-Powered Desalination Plants: A Sustainable Alternative Water-Energy Nexus to Obtain Water for Chile's Coastal Areas. Energies. 2022 Dec 6;15(23):9245.

[12] Borba ATA, Simões LJM, de Melo TR, Santos AÁB. Techno-Economic Assessment of a Hybrid Renewable Energy System for a County in the State of Bahia. Energies. 2024 Jan 24;17(3):572.

[13] Gökçek M. Integration of hybrid power (wind-photovoltaic-diesel-battery) and seawater reverse osmosis systems for small-scale desalination applications. Desalination. 2018 Jun;435:210–20.
[14] Hasan SMN, Ahmad S, Liaf AF, Mustayen AGMB, Hasan MM, Ahmed T, et al. Techno-Economic Performance and Sensitivity Analysis of an Off-Grid Renewable Energy-Based Hybrid System: A Case Study of Kuakata, Bangladesh. Energies. 2024 Mar 19;17(6):1476.
[15] Ramazanian S, Aliehyaei M, Salimi M, Najafizadeh MM. Theoretical and experimental investigation of reverse osmosis (RO) desalination solar system using the solar panel, battery, and water turbine for high-pressure recovery of output brine. Sol Energy. 2023 Sep;262:111852.
[16] Abdelrahman MA, Sallam GR, Dawoud MA, Sakr RY, Emam M. Improving the performance of a PV-RO brackish water desalination plant in Egypt using solar thermal feed preheating technology. J Energy Storage. 2024 Sep;98:113115.
[17] Monnot M, Carvajal GDM, Laborie S, Cabassud C, Lebrun R. Integrated approach in eco-design strategy for small RO desalination plants powered by photovoltaic energy. Desalination. 2018 Jun;435:246–58.
[18] Elmaadawy K, Kotb KM, Elkadeem MR, Sharshir SW, Dán A, Moawad A, et al. Optimal sizing and techno-enviro-economic feasibility assessment of large-scale reverse osmosis desalination powered with hybrid renewable energy sources. Energy Convers Manag. 2020 Nov;224:113377.
[19] Ali FAA. Optimizing size and evaluating Techno-Enviro-Economic Feasibility of hybrid renewable energy to power RO/Well unit. Results Eng. 2024 Sep;23:102805.
[20] He WF, Han D, Ji C. Investigation on humidification dehumidification desalination system coupled with heat pump. Desalination. 2018 Jun;436:152–60.
[21] Giwa A, Fath H, Hasan SW. Humidification–dehumidification desalination process driven by photovoltaic thermal energy recovery (PV-HDH) for small-scale sustainable water and power production. Desalination. 2016 Jan;377:163–71.
[22] Luberti M, Capocelli M. Enhanced Humidification–Dehumidification (HDH) Systems for Sustainable Water Desalination. Energies. 2023 Sep 1;16(17):6352.
[23] Abdelgaied M, Kabeel AE, Kandeal AW, Abosheiasha HF, Shalaby SM, Hamed MH, et al. Performance assessment of solar PV-driven hybrid HDH-RO desalination system integrated with energy recovery units and solar collectors: Theoretical approach. Energy Convers Manag. 2021 Jul;239:114215.
[24] Abdullah AS, Aljaghtham M, Kandeal AW, Sharshir SW. Techno-economic investigation of an entirely solar-powered hybrid HDH/RO desalination plant for moderate water demand under various operating conditions. Results Eng. 2024 Dec;24:103200.
[25] Suresh V, M. M, Kiranmayi R. Modelling and optimization of an off-grid hybrid renewable energy system for electrification in a rural areas. Energy Reports. 2020 Nov;6:594–604.
[26] Bazdar E, Shirzadi N. Economic Analysis and Simulation of Solar PV, Wind Turbine Hybrid Energy System Using HOMER pro. J Sol Energy Res. 2017;2(3):53–8.
[27] Prasetyo SD, Pranata BBP, Alfaridzi MS, Arifin Z, Harsito C, Mauludin MS, et al. Techno-Economic Assessment of Solar Power Plants on River Land in Indonesia Using HOMER Pro. J Urban Dev Manag. 2024 Jul 23;3(3):164–75.
[28] Shahzad MK, Zahid A, ur Rashid T, Rehan MA, Ali M, Ahmad M. Techno-economic feasibility analysis of a solar-biomass off grid system for the electrification of remote rural areas in Pakistan using HOMER software. Renew Energy. 2017 Jun;106:264–73.
[29] Adetoro SA, Ndubuka Nwohu M, Olatomiwa L. Techno-economic Analysis of Hybrid Energy System Connected to an Unreliable Grid: A Case Study of a Rural Community in Nigeria. In: 2022 IEEE Nigeria 4th International Conference on Disruptive Technologies for Sustainable

Development (NIGERCON). IEEE; 2022. p. 1–5.

[30] Ibrahim MM, Mostafa NH, Osman AH, Hesham A. Performance analysis of a stand-alone hybrid energy system for desalination unit in Egypt. Energy Convers Manag. 2020 Jul;215:112941.

[31] Cristian H, Bizon N, Alexandru B. Design of hybrid power systems using HOMER simulator for different renewable energy sources. In: 2017 9th International Conference on Electronics, Computers and Artificial Intelligence (ECAI). IEEE; 2017. p. 1–7.

[32] Rey AL, Santiago RVM, Pacis MC. Modeling of a hybrid renewable power system for Calayan Island, Cagayan using the HOMER software. In: 2017IEEE 9th International Conference on Humanoid, Nanotechnology, Information Technology, Communication and Control, Environment and Management (HNICEM). IEEE; 2017. p. 1–6.

[33] Elsayed I, Kanaan H, Mehanna M. Feasibility and optimal sizing analysis of hybrid PV/Wind powered seawater desalination system: A case study of four ports, Egypt. Heliyon. 2024 Nov;10(22):e40313.

[34] Bouseba L, Chaker A. Implementing of a grid-connected PV energy system in building with medium consumption: A techno- economic case study. Energy Build. 2024 Dec;324:114929.

[35] Clarke DP, Al-Abdeli YM, Kothapalli G. Multi-objective optimisation of renewable hybrid energy systems with desalination. Energy. 2015 Aug;88:457–68.

[36] Brandoni C, Bošnjaković B. HOMER analysis of the water and renewable energy nexus for water-stressed urban areas in Sub-Saharan Africa. J Clean Prod. 2017 Jul;155:105–18.

[37] Mostafaeipour A, Qolipour M, Rezaei M, Babaee-Tirkolaee E. Investigation of off-grid photovoltaic systems for a reverse osmosis desalination system: A case study. Desalination. 2019 Mar;454:91–103.

[38] Atallah MO, Farahat MA, Lotfy ME, Senjyu T. Operation of conventional and unconventional energy sources to drive a reverse osmosis desalination plant in Sinai Peninsula, Egypt. Renew Energy. 2020 Jan;145:141–52.

[39] Cherif H, Belhadj J, Champenois G. Intelligent optimization of a hybrid renewable energy system-powered water desalination unit. Int J Environ Sci Technol. 2021 Nov 5;18(11):3539–52.

[40] Karimi L, Abkar L, Aghajani M, Ghassemi A. Technical feasibility comparison of off-grid PV-EDR and PV-RO desalination systems via their energy consumption. Sep Purif Technol. 2015 Sep;151:82–94.

[41] Halabi LM, Mekhilef S, Olatomiwa L, Hazelton J. Performance analysis of hybrid PV/diesel/battery system using HOMER: A case study Sabah, Malaysia. Energy Convers Manag. 2017 Jul;144:322–39.

[42] Al Garni HZ, Awasthi A, Ramli MAM. Optimal design and analysis of grid-connected photovoltaic under different tracking systems using HOMER. Energy Convers Manag. 2018 Jan;155:42–57.

[43] Zahboune H, Zouggar S, Yong JY, Varbanov PS, Elhafyani M, Ziani E, et al. Modified Electric System Cascade Analysis for optimal sizing of an autonomous Hybrid Energy System. Energy. 2016 Dec;116:1374–84.

[44] Behmounesi SA, Saraei A, Afshar H, Ashtiani HAD, Dehghani-Sanij A. Techno-economic analysis of optimally hybrid photovoltaic-wind systems to meet the energy demand of a residential building in six different areas of Iran. Energy Convers Manag. 2024 Dec;322:119131.

[45] Winsly BW, Ramalingam VK, Santhappan JS, Maria AJ, Chokkalingam MP, Rajendran V. Optimal sizing and techno-economic-environmental evaluation of biomass-solar-wind-grid hybrid energy system: A case study of an institute in South India. Energy Convers Manag. 2025 Feb;325:119352.

[46] Schär S, Bischi A, Baccioli A, Desideri U, Geldermann J. Optimization of sustainable seawater desalination: Modeling renewable energy integration and energy storage concepts. Energy Convers Manag. 2023 Oct;293:117447.

[47] Yang Y, Yang R, Chen X, Ma X, Yu S, Liu S, et al. Design and thermo-

environmental analysis of a novel solar-driven system integrating desalination, photocatalytic water splitting, and fuel cell technologies. Energy Convers Manag. 2025 Jan;323:119271.

[48] Safarzadeh Ravajiri E, Jalali A, Houshfar E. Multi-objective optimization and 4E analysis of an integrated system based on waste-to-energy, solar PV, power-to-gas, and HDH-RO desalination. Energy Convers Manag. 2023 Feb;277:116677.

[49] Abdala AMM, Elwekeel FNM, Taccani R. The Effect of Hydrogen as a Coolant on the Characteristics of Humidification-Dehumidification Desalination Systems. Energies. 2024 Jul 22;17(14):3593.

[50] Jamil MA, Elmutasim SM, Zubair SM. Exergo-economic analysis of a hybrid humidification dehumidification reverse osmosis (HDH-RO) system operating under different retrofits. Energy Convers Manag. 2018 Feb;158:286–97.

[51] Abooei Koochaksaraei S, Behzadi-Sarok M, Saidi MH. Thermal, Exergy, and Economic Analysis of Humidification-Dehumidification Desalination System Assisted by Heat Pump (Hdh-Hp) Using the Poppe Method at Different Salinities. Separation and Purification Technology. Elsevier; 2025. p. 133284.

[52] Behzadi-Sarok M, Saidi MH, Shafii M behshad. Experimental Thermal Investigation of Bubble Column Humidification-Dehumidification (Bc-Hdh) Desalination Combined with Submerged Type Water Source Heat Pump (Wshp) for Different Salinities . 2024.

[53] Behzadi-Sarok M, Saidi MH. Thermal investigation of humidification process using the Poppe method, a semi-analytical method. Int J Thermofluids. 2025 Sep;29:101369.

[54] Behzadi-Sarok M, Saidi MH, Shafii MB. Design and off-design analysis of a heat pump assisted humidification-dehumidification (HDH HP) desalination system for a wide range of salinities. Int J Refrig. 2025 Mar;171:147–64.

[55] Diouf B, Pode R. Potential of lithium-ion batteries in renewable energy. Renew Energy. 2015 Apr;76:375–80.

[56] von Srbik M, Wu B, Offer GJ, Yufit V, Marinescu M. The effect of thermal gradients on the performance of battery packs in automotive applications. In: Hybrid and Electric Vehicles Conference 2013 (HEVC 2013). Institution of Engineering and Technology; 2013. p. 1.1-1.1.

[57] Araki T, Wakahara K, Fukuda K, Ohmori Y, Nakayama M, Onda K. Thermal Behavior of Prismatic Lithium-Ion Battery during Rapid Charge and Discharge Cycles. IEEJ Trans Power Energy. 2005;125(12):1332–7.

[58] Seong Kim U, Yi J, Shin CB, Han T, Park S. Modeling the Dependence of the Discharge Behavior of a Lithium-Ion Battery on the Environmental Temperature. J Electrochem Soc. 2011;158(5):A611.

[59] Kim US, Yi J, Shin CB, Han T, Park S. Modeling the Thermal Behaviors of a Lithium-Ion Battery during Constant-Power Discharge and Charge Operations. J Electrochem Soc. 2013 Apr 23;160(6):A990–5.

[60] Li Y, Zhou Z, Su L, Bai M, Gao L, Li Y, et al. Numerical Simulations for Indirect and Direct Cooling of 54 V LiFePO4 Battery Pack. Energies. 2022 Jun 23;15(13):4581.

[61] Li K, Sun C, Zhang M, Wang S, Wei B, Cheng Y, et al. A Study of the Thermal Management and Discharge Strategies of Lithium-Ion Batteries in a Wide Temperature Range. Energies. 2024 May 11;17(10):2319.

[62] NASA. Available from: https://power.larc.nasa.gov

[63] Bergman TL, Lavine AS, Incropera FP, DeWitt DP. Introduction to heat transfer. John Wiley & Sons; 2011.